

1 Evaluation of Re-Os geochronology and Os isotope fingerprinting of Late
2 Cretaceous terrestrial oils in Taranaki Basin, New Zealand

3 Enock K. Rotich^{a*}, Monica R. Handler^a, Richard Sykes^b, Sebastian Naeher^b, David
4 Selby^c, Karsten Kroeger^b

5
6 ^a *School of Geography, Environment and Earth Sciences, Victoria University of Wellington,*
7 *PO Box 600, Wellington, 6140, New Zealand*

8 ^b *GNS Science, 1 Fairway Drive, PO Box 30368, Lower Hutt, 5040, New Zealand*

9 ^c *Department of Earth Sciences, Durham University, Durham, DH1 3LE, UK*

10

11

12

13

14

15

16

17

18

19

20

21

22 * Corresponding author. Tel.: +254768268931; e-mail address: rotichenock@gmail.com

23 **Abstract**

24 The rhenium-osmium (Re-Os) isotope system has been applied to several marine and
25 lacustrine petroleum systems worldwide, showing good potential for dating crude oils
26 and correlating them to their source rocks. Here we explore the applicability of the Re-
27 Os geochronometer and Os isotope fingerprinting to terrestrial oils by comparing the
28 Re and Os systematics of Late Cretaceous terrestrial oils from Taranaki Basin, New
29 Zealand, and their correlated coaly source rocks. Comparison is also made with
30 selected Late Cretaceous–Paleocene marine oils and source rocks with varying levels
31 of terrestrial organic matter input.

32 The asphaltene fractions of nine genetically related terrestrial oils from the Maui,
33 Maari-Manaia and Tui Area fields in offshore Taranaki Basin contain low
34 concentrations of Re (0.18–0.45 ppb) and ^{192}Os (1.3–12.7 ppt) comparable to their
35 correlated Late Cretaceous coaly source rocks (Rakopi and North Cape formations;
36 Re 0.19–0.37 ppb, ^{192}Os 5.3–9.6 ppt). The Re and ^{192}Os concentrations in these
37 terrestrial oils are generally one to two orders of magnitude lower than those in marine-
38 sourced oils from the Kora Field in offshore Taranaki Basin and surface seeps in East
39 Coast Basin.

40 The $^{187}\text{Re}/^{188}\text{Os}$ and $^{187}\text{Os}/^{188}\text{Os}$ ratios of the terrestrial oils failed to yield a precise
41 Re-Os isochron age. We attribute this to: (1) insufficient homogenisation of oils with
42 widely variable initial $^{187}\text{Os}/^{188}\text{Os}$ (Os_i) values inherited from thick, coaly source rock
43 intervals (up to about 2700 m) within the Maui sub-basin and northern Kahurangi
44 Trough kitchens; (2) insufficient spread of $^{187}\text{Re}/^{188}\text{Os}$ values (only 275 units); (3)
45 insufficient time since oil expulsion (modelled to be from approximately 10 Ma to the
46 present day) for the evolution of an isochron; and (4) possible effects of water washing
47 of the oil columns. Although all of the studied oils are water-washed to varying

48 degrees, there is no definitive evidence that water washing has disturbed the Re-Os
49 systematics.

50 The O_s values for the studied terrestrial oils inherited at the modelled time of oil
51 expulsion (approximately 10 Ma) display a wide range (0.47–1.14) and do not provide
52 a unique fingerprint of their Late Cretaceous coaly source rock formations. Osmium
53 isotope compositions therefore appear to have limited potential for broad oil-source
54 rock correlation within the predominantly coal-sourced petroleum systems of Taranaki
55 Basin. The O_s values may, however, provide useful distinction of the terrestrial oils
56 emanating from the Kahurangi Trough (Tui Area oils) from those of the Maui sub-basin
57 (Maui and Maari-Manaia oils) based on the significantly more radiogenic values of the
58 Tui Area oils (0.84–1.14 compared with 0.47–0.65 from Maui and Maari-Manaia oils).
59 Overall, this study has provided useful insights into the potential application of the Re-
60 Os isotope system to terrestrial, coal-sourced petroleum systems.

61

62 **Keywords**

63 Re-Os isotopes; terrestrial oils; marine oils; seeps; coaly source rocks; Taranaki Basin;
64 East Coast Basin; New Zealand

65

66 **1. Introduction**

67 The Re-Os isotope system has been shown to provide accurate and precise
68 depositional ages for both marine and lacustrine organic-rich mudrocks (e.g., Cohen
69 et al., 1999; Xu et al., 2009; Cumming et al., 2012; Liu et al., 2018; Tripathy et al.,
70 2014; Rotich et al., 2020). Prerequisites for valid ages are: 1) the Re-Os isotope
71 systematics must remain a closed system, 2) the initial $^{187}\text{Os}/^{188}\text{Os}$ (O_s) compositions

72 of all samples must be similar, and 3) there must be a sufficient spread in $^{187}\text{Re}/^{188}\text{Os}$
73 ratios to define an isochron (Cohen et al., 1999; Cumming et al., 2012). Additionally,
74 studies of natural systems and hydrous pyrolysis experiments have shown that Re
75 and Os are transferred from source rocks to bitumen to oil without significant
76 fractionation, and without significantly affecting Re-Os systematics and Os isotopic
77 composition of the source rock (Selby et al., 2007; Finlay et al., 2012; Rooney et al.,
78 2012; Cumming et al., 2014). Accordingly, the Re-Os geochronometer and Os isotope
79 fingerprinting have shown promising potential both for dating crude oils in marine and
80 lacustrine petroleum systems and for correlating oils to their source rocks (Selby and
81 Creaser, 2005; 2007; Finlay et al., 2011; 2012; Lillis and Selby, 2013; Cumming et al.,
82 2014; Georgiev et al., 2016; 2019; Ge et al., 2018; Liu et al., 2018; Corrick et al., 2019;
83 Scarlett et al., 2019; Meng et al., 2021). However, it remains uncertain exactly which
84 event is being dated. Some studies have linked crude oil Re-Os isochron ages and
85 $^{187}\text{Os}/^{188}\text{Os}$ compositions to the timing of oil generation (e.g., Finlay et al., 2011;
86 Cumming et al., 2014; Liu et al., 2018), whereas others have linked them to both oil
87 generation and migration (e.g., Lillis and Selby, 2013; Ge et al., 2016; 2018) or oil
88 emplacement (Selby and Creaser, 2005), as identified independently by other age
89 estimation techniques, such as basin modelling and paleomagnetic and radiometric
90 dating (Ar-Ar, U-Pb, Rb-Sr) of hydrocarbon-bearing fluid inclusions and mineral
91 deposits (Christensen et al., 1995; Symons and Arne, 2003; Mark et al., 2010; Lillis
92 and Selby, 2013; Ge et al., 2016; 2018).

93 The lack of clarity on the event being dated can be attributed to the significant gaps in
94 existing knowledge of the geochemical behaviour and mechanisms that control
95 fractionation of Re and Os in petroleum systems, especially the homogenization of Os
96 isotope composition. For Re-Os hydrocarbon geochronology to work, a complete reset
97 of the isotopic system must happen either during generation, migration or

98 accumulation, and the system must remain closed throughout subsequent geological
99 time. Most Re-Os hydrocarbon dates obtained so far are not precise enough to clearly
100 distinguish the exact process being dated. Hydrous pyrolysis experiments simulating
101 hydrocarbon generation (Rooney et al., 2012; Cumming et al., 2014) show that, at a
102 local scale, this process is capable of homogenising osmium isotopes as well as
103 fractionating Re/Os ratios, the two conditions necessary for development of an
104 isochron. Experiments have also been conducted to assess the effects of sequential
105 precipitation of asphaltenes on fractionation of Re/Os ratios during migration and
106 charging of oil into reservoirs (Mahdaoui et al., 2013; DiMarzio et al., 2018; Liu et al.,
107 2019). Results show that this process does not appreciably perturb the Re-Os
108 geochronometer, especially when the precipitation of asphaltene is minimal.
109 Interaction of crude oil with formation water and hydrothermal fluids is another
110 potential mechanism that can reset the Re-Os geochronometer as has been shown
111 by oil-water contact experiments (Mahdaoui et al., 2015; Hurtig et al., 2019) and
112 reported in natural systems (Finlay et al., 2010). The oil-water contact experiments
113 reveal that Re and Os can readily transfer from aqueous solutions to oils, especially
114 at high water-oil ratios. Thermal cracking is another process that may reset Re-Os
115 isotope systematics in crude oils, resulting in oil isochrons that record the timing of
116 thermal cracking (production of dry gas and pyrobitumen), rather than generation or
117 migration of oil (Lillis and Selby, 2013; Ge et al., 2016). Similarly, thermochemical
118 sulfate reduction (TSR) has been shown to have caused a reset of the Re-Os
119 geochronometer in oils from the Bighorn Basin, USA, yielding a Re-Os date of $9.24 \pm$
120 0.39 Ma, which coincides with the proposed end of TSR as a result of reservoir cooling
121 caused by uplift and erosion at around 10 Ma (Lillis and Selby, 2013).

122 The comprehensive studies of the Eocene lacustrine Green River Formation source
123 rocks (Cumming et al., 2012) and their derived oils, tar sands and gilsonite deposits

124 (Cumming et al., 2014) further highlight some of the challenges and uncertainties in
125 Re-Os dating of petroleum systems. While the oils and gilsonite deposits returned
126 Middle Eocene Model 3 isochron ages of 45 ± 31 Ma and 45 ± 42 Ma, respectively,
127 consistent with the range of Re-Os and Ar-Ar depositional dates for the Green River
128 Formation (45.4–50.1 Ma; Cumming et al., 2012), regression of all the samples (oils,
129 gilsonites and tar sands) yielded an isochron age of 19 ± 14 Ma, broadly consistent
130 with a petroleum generation age of ~ 25 Ma derived from basin models. The large
131 uncertainties in the Re-Os ages of the various petroleum deposits were attributed
132 mainly to very low Os abundances, limited spread in measured $^{187}\text{Re}/^{188}\text{Os}$ and
133 $^{187}\text{Os}/^{188}\text{Os}$ ratios, and wide variation in initial $^{187}\text{Os}/^{188}\text{Os}$ compositions, the latter
134 exacerbated by multiple generation events occurring through a ~ 3000 m-thick source
135 rock unit (Cumming et al., 2014).

136 The applicability of the Re-Os isotope system to date and trace crude oils derived from
137 terrestrial (coaly) source rocks has not yet been tested. Terrestrial petroleum systems
138 rarely attain the levels of Os_i homogeneity commonly seen in marine petroleum
139 systems. This is because the source materials for terrestrial source rocks (i.e., detrital
140 silicates and plant debris) have been shown to exhibit heterogeneous Os isotope
141 compositions (Rodushkin et al., 2007; Goswami et al., 2018), and were deposited in
142 bogs or mires far smaller and more restricted than depocenters in the open ocean.
143 Such depositional settings prevent complete mixing and homogenisation of the Os
144 isotope signature before sequestration. Recent studies have indeed provided
145 evidence of heterogeneous initial $^{187}\text{Os}/^{188}\text{Os}$ ratios in coaly source rocks (Goswami
146 et al., 2018; Rotich et al., 2021). Such variable initial $^{187}\text{Os}/^{188}\text{Os}$ ratios may be
147 transferred to crude oils during maturation, potentially hindering the application of Re-
148 Os geochronology to terrestrial oils. However, the processes that homogenise Os
149 isotopic composition in marine and lacustrine crude oils, such as primary migration

150 (Selby and Creaser, 2005), should also apply to coal-sourced oils. In addition, the Os
151 isotopic compositions of these oils may prove useful for oil-source correlation,
152 provided estimates of oil expulsion dates are available through other means, such as
153 basin modelling.

154 In this study, we explore the possibility of using the Re-Os isotope system to date and
155 trace selected terrestrial oils from offshore Taranaki Basin, New Zealand (Figs 1, 2).
156 These oils have been confidently typed to Late Cretaceous coaly source rocks of the
157 Rakopi and North Cape formations using biomarker compounds (Killops et al., 1994;
158 Sykes et al., 2012; Sykes, 2019). Using results of a previous study of the Re-Os
159 systematics of these source rocks (Rotich et al., 2021) allows us to also assess the
160 potential of Os isotope fingerprinting to correlate terrestrial oils to their source rocks.
161 Further, we investigate the effects of terrestrial organic matter input on the Re-Os
162 isotope system by comparing the Re-Os results for these coal-sourced oils with those
163 for two families of marine oils that differ in their levels of terrestrial organic matter input.
164 The highly distinctive marine oils from the Kora-1 well in northern offshore Taranaki
165 Basin (Fig. 1) are sourced from organic-rich mudstones of the late Paleocene, marine
166 Waipawa Formation (Killops et al., 1994; Sykes et al., 2012), which are very rich in
167 transported terrestrial organic matter (e.g., Schiøler et al., 2010; Field et al., 2018;
168 Naeher et al., 2019). In contrast, the marine seep oils of the northern and southern
169 regions of onshore East Coast Basin (Fig. 1) are more typical marine oils characterised
170 by little terrestrial organic matter input. These seep oils are from an as-yet unknown
171 source, but have biomarker and carbon isotopic characteristics similar to those of the
172 Late Cretaceous–Paleocene Whangai Formation (Murray et al., 1994; Killops, 1996;
173 Rogers et al., 1999; Sykes et al., 2012). The Re-Os isotope systematics of Waipawa
174 and Whangai Formation mudstones have previously been characterised (Rotich et al.,

175 2020), enabling comparison of the Kora-1 and East Coast Basin seep oils with these
176 source rocks.

177 **2. Geological setting**

178 New Zealand crude oils (including gas condensates) have been grouped into five
179 genetic tribes and 11 families based on chemometric analysis of source-related
180 biomarker and carbon isotope parameters (Sykes et al., 2012). Nine families of
181 terrestrial oils are distinguished mainly by their relative inputs of angiosperm-,
182 gymnosperm- and total higher plant-derived organic matter to the source kerogen, as
183 well as the degree of marine influence within the coal-forming depositional
184 environment. The two marine oil families are distinguished primarily by their carbon
185 isotope signatures and C₃₀ sterane contents (Killops et al., 1994; Murray et al., 1994;
186 Killops, 1996; Rogers et al., 1999; Sykes et al., 2012). This study investigates oil
187 accumulations in Taranaki Basin correlated to Late Cretaceous terrestrial source rocks
188 (Family 11) and late Paleocene, marine Waipawa Formation source rocks (Family 41),
189 as well as seep oils in East Coast Basin (Family 42) with source characteristics similar
190 to the Late Cretaceous–Paleocene, marine Whangai Formation (Figs. 1, 2).

191 **2.1. Taranaki petroleum systems**

192 Taranaki Basin is the only oil and gas producing basin in New Zealand, with estimated
193 ultimate recoverable reserves of 600 million barrels of oil and condensate and 8.7
194 trillion cubic feet of gas (MBIE, 2020). The basin covers approximately 330,000 km²
195 both onshore and offshore along the west coast of New Zealand's North Island (Figs.
196 1, 2) and comprises up to 10 km of mid-Cretaceous to recent sedimentary rocks (King
197 and Thrasher, 1996). The main petroleum source rocks are mid-Cretaceous–Eocene
198 coal measures deposited in extensive coastal plain environments. These source rocks
199 were buried to depths sufficient for oil and gas generation and expulsion in the

200 Neogene (King and Thrasher, 1996; Kroeger et al., 2016). Commercial petroleum
201 accumulations have been encountered at every stratigraphic level from the Paleocene
202 to Pliocene (King and Thrasher, 1996). Most accumulations are trapped in fault-related
203 anticlines that formed in the last 30 to 40 Myr in response to compression associated
204 with subduction of the Pacific Plate to the east of New Zealand (King and Thrasher,
205 1996; Stagpoole and Nicol, 2008; Reilly et al., 2016; Seebeck et al. 2019; Kroeger et
206 al., 2021).

207 There are currently 17 producing oil and gas-condensate fields in Taranaki Basin, both
208 on- and offshore (MBIE, 2020). The Family 11 oils studied here are from the offshore
209 Maui, Maari-Manaia and Tui Area fields (Fig. 2), and all have high contents of
210 gymnosperm plant-derived biomarkers that link them to Late Cretaceous coaly rocks
211 of the Rakopi and North Cape formations (Killops et al., 1994; Sykes et al., 2012;
212 Sykes, 2019). These coaly rocks span a wide range of total organic carbon (TOC)
213 from <1% to about 80% and hydrogen index (HI) values are mostly in the range of
214 200–450 mg HC/g TOC (Sykes and Zink, 2018), indicating high quality, mixed gas-
215 and oil-prone to oil-prone kerogen (classification of Peters and Cassa, 1994). Regional
216 geological models and seismic facies maps indicate these source rocks are present in
217 depocenters of the Maui and Pihama sub-basins to the east, and the Kahurangi
218 Trough to the west (Funnell et al., 2001; 2004; Matthews, 2008; Kroeger et al., 2016;
219 2021; Fig. 2). Late Cretaceous strata within these depocentres are up to c. 2700 m
220 thick (Seebeck et al., 2019) and are modelled to have been generating and expelling
221 significant quantities of oil and gas from the Late Miocene to the present (Killops et al.,
222 1994; Funnell et al., 2004; Harrison et al., 2013; Kroeger et al., 2016; Pierpont et al.,
223 2017). These hydrocarbons are trapped in Paleocene–Miocene, stacked terrestrial
224 and marine sandstone reservoirs, commonly referred to as the F, D, C and B sands
225 (King and Thrasher, 1996; Funnell et al., 2004). The Paleocene F sands (within the

226 Farewell Formation) and Early Eocene D sands (Kaimiro Formation) were deposited
227 in nearshore, paralic and fluvio-estuarine environments (Higgs et al. 2012). The
228 Middle–Late Eocene C sands (Mangahewa Formation) consist of coastal plain,
229 shoreface, tidal channel and inner shelf sediments, whereas the Middle Miocene B
230 sands (Moki Formation) comprise basin floor, slope turbidite and channel sandstones
231 (King and Thrasher, 1996; Funnell et al., 2004; Higgs et al. 2012; Kroeger et al. 2019).

232 In the northern part of Taranaki Basin, sub-commercial oil accumulations were
233 discovered in the Kora-1 well that was drilled to target a Miocene-aged submarine
234 volcano (King and Thrasher, 1996; Brett, 2005; Bischoff et al. 2021, Kroeger et al.,
235 2022). These oils are assigned to Family 41 and are geochemically correlated with the
236 late Paleocene Waipawa Formation whose organic matter is derived from both
237 terrestrial higher plants and marine algae (Reed, 1992; Killops et al., 1994; Murray et
238 al., 1994; Killops, 1996; Clayton, 2011; Sykes et al., 2012; Naeher et al., 2019). The
239 Waipawa Formation is primarily gas-condensate-prone on account of its large
240 proportion of terrestrial organic matter, dominated (66–98%) by woody phytoclasts
241 (Naeher et al., 2019). Nonetheless, its strong geochemical correlation with the Kora
242 oils and a number of oil seeps and stains in the southern Hawke’s Bay to Wairarapa
243 region of East Coast Basin (Fig. 1) indicates some oil potential, presumably from
244 subordinate contributions of marine, algal-derived kerogen. The two principal reservoir
245 units in the Kora Field are the Eocene Tangaroa Formation, which comprises deep-
246 water submarine fan sandstones, and volcanoclastic rocks intercalated in the Miocene
247 Mohakatino Formation (Reed, 1992; Brett, 2005; Bischoff et al. 2021).

248 **2.2. East Coast Basin petroleum systems**

249 East Coast Basin is located both on- and offshore along the eastern margin of North
250 Island and northeastern South Island, covering about 120,000 km² (Fig. 1). The basin

251 has numerous onshore oil and gas seeps and stains indicating the presence of active
252 petroleum systems (Field et al., 1997). Late Cretaceous–Paleocene carbonaceous
253 mudstones of the marine Whangai and Waipawa formations have been identified as
254 the most promising source rocks, although no commercial accumulations of oil or gas
255 linked to either formation have yet been discovered in the basin (Field et al., 1997;
256 Hollis and Manzano-Kareah, 2005). The Waipawa Formation has a maximum known
257 thickness within the basin of c. 80 m and has relatively high TOC contents, averaging
258 3.6 wt.% (n=99), and moderate HI values, averaging 245 mg HC/g TOC (n=87; Hollis
259 and Manzano-Kareah, 2005; Field et al., 2018). These values indicate very good
260 potential for mixed oil and gas. The formation appears thermally immature to
261 marginally mature throughout at least the onshore part of the basin (Moore, 1989; Field
262 et al., 1997; Hollis and Manzano-Kareah, 2005), where it has been geochemically
263 linked to minor oil seeps and stains assigned to Family 41 in the southern Hawke's
264 Bay and Wairarapa regions (Fig. 1, Murray et al., 1994; Killops, 1996; Rogers et al.,
265 1999). Both the Waipawa and Whangai formations are, however, modelled to have
266 higher thermal maturities offshore, in the Hikurangi subduction margin (Kroeger et al.,
267 2015).

268 The Whangai Formation is up to c. 1500 m thick and appears to have generally poor
269 to fair potential for gas only (Hollis and Manzano-Kareah, 2005). Overall, Whangai
270 Formation carbonaceous mudstones have mean TOC and HI values of 0.56 wt.%
271 (n=284) and 159 mg HC/g TOC (n=188), respectively, although individual values are
272 as high as 1.7 wt.% and 377 mg HC/g TOC (Hollis and Manzano-Kareah, 2005).
273 Multiple seep oils in the Raukumara Peninsula and Marlborough regions of the
274 northern and southern onshore East Coast Basin (Fig. 1), respectively, including the
275 Waitangi and Kaikoura seep oils studied here, are assigned to Family 42, with source
276 organofacies characteristics similar to those of the Whangai Formation (Rogers et al.,

277 1999; Sykes et al., 2012). However, given the generally low oil potential of this
278 formation, it remains uncertain whether these oils were sourced from an as-yet-
279 undiscovered oil-prone organofacies within the Whangai Formation or from a
280 separate, as-yet-unknown Cretaceous formation with similar source organofacies
281 characteristics.

282 **3. Samples and methods**

283 **3.1. Oil samples**

284 **3.1.1. Origin of samples**

285 Thirteen oil samples representative of the coal-sourced Family 11 and marine-sourced
286 families 41 and 42 were selected from a collection of oils held at GNS Science, Lower
287 Hutt, and the National Core Store, Featherston, New Zealand (Table 1). The nine
288 Family 11 oils are from the Maui, Maari-Manaia and Tui Area fields, which are spread
289 over c. 75 km across the offshore Taranaki Basin (Fig. 2). The Maui and Tui Area oils
290 are from the Paleocene and Eocene F and D sands reservoirs, whereas the Maari-
291 Manaia oils are from the much shallower, Miocene B sands reservoir. The Tui Area
292 fields consist of three separate, c. 10–12 m thick oil accumulations, forming the
293 Pateke, Amokura and Tui pools (Fig. 2), all within the same F10 sand. These pools
294 represent a fill-spill chain shallowing to the south (i.e. from Pateke to Tui) over a lateral
295 distance of c. 10 km (Matthews et al., 2008). The Maui B well oil sample is also from
296 the F sands, whereas the Maui-1 well oil is from the D sands. The marine Family 41
297 oils are from the two different reservoirs penetrated in the Kora-1 discovery well in
298 northern offshore Taranaki Basin (Fig. 1; Reed, 1992). The Kora-1(A) oil is from the
299 Eocene Tangaroa Formation sandstone reservoir whereas the Kora-1(B) oil is from
300 the Miocene Mohakatino Formation reservoir comprising volcanoclastic sediments.
301 The marine Family 42 oil samples are from the Waitangi and Kaikoura surface seeps

302 in the Raukumara Peninsula and Marlborough regions of northern and southern East
303 Coast Basin, respectively (Fig. 1).

304 **3.1.2. Oil sample properties and quality**

305 All of the oil samples studied here have previously been analysed for their bulk
306 compound groups (i.e., saturated and aromatic hydrocarbons, resins and
307 asphaltenes), whole-oil hydrocarbon distributions, saturated and aromatic biomarkers,
308 and stable carbon isotope compositions of the saturated and aromatic hydrocarbon
309 fractions (Sykes and Zink, 2018; GNS Science unpublished results). This enabled
310 initial selection of samples based on the assigned oil family, oil quality and asphaltene
311 content. Asphaltene content is considered important for sample selection because the
312 asphaltene fraction typically contains the majority (up to 98%) of the Re and Os in
313 crude oils (Selby et al., 2007; Georgiev et al., 2016; Liu et al., 2019), but New Zealand
314 coal-sourced oils are typically low in asphaltenes (<3%; Sykes and Zink, 2018).
315 Sample selection therefore favoured those oils with higher asphaltene contents.

316 Studies of the Re-Os isotope system and geochronology of crude oils should ideally
317 use pristine oils that are unaltered from the original oil that charged the host reservoirs.
318 However, crude oils are commonly altered by processes such as biodegradation and
319 water washing, either within the reservoir or surface seeps (Peters et al., 2005, and
320 references therein). In addition, oil samples are typically missing some volatile low
321 molecular weight hydrocarbons (i.e., “front-ends”) as a result of less-than-ideal sample
322 collection and storage procedures. While the loss of volatiles is unlikely to have a
323 significant impact on the Re and Os budget, this may not be the case with
324 biodegradation and water washing. Biodegradation is the alteration of crude oil by
325 microbial organisms primarily through the process of oxidation which produces carbon
326 dioxide and other partially oxidized by-products, such as organic acids (Peters et al.,

2005). For biodegradation to occur, specific conditions that support microbial life must exist. These include reservoir temperatures of less than $\sim 80^{\circ}\text{C}$, availability of water and inorganic nutrients, water salinity of less than $\sim 100\text{--}150$ parts per thousand and presence of microorganisms (Wenger et al., 2002; Peters et al., 2005; Wang et al., 2016). A scale of 1 (least altered) to 10 (most altered) has been developed to rank the extent of biodegradation of crude oil based on differing resistance of its components to microbial attack (Peters and Moldowan, 1993; Peters et al., 2005). On this scale, level 1 is assigned to slightly biodegraded oils, level 2 to moderately biodegraded oils, level 3 to heavily biodegraded oils and levels 4–10 to severely biodegraded oils (Peters et al., 2005). Water washing is the removal of the more water-soluble constituents of crude oil, especially light alkanes and low molecular weight aromatic hydrocarbons such as benzene and toluene (Palmer, 1984). It occurs when crude oils come in contact with water in reservoirs, during migration and/or during production. Water washing is an important consideration in Re-Os studies of crude oils because contact experiments have demonstrated that Re and Os can readily transfer between aqueous solutions and oils (Mahdaoui et al., 2015; Hurtig et al., 2019), raising the possibility that mixing of oil with formation or surface waters may disturb the Re-Os systematics (Finlay et al., 2010).

The Tui Area and Maui B oils have *n*-alkane distributions typical of largely unaltered New Zealand coal-sourced oils apart from the usual loss of some gas- ($\text{C}_1\text{--}\text{C}_4$) and gasoline-range ($\text{C}_5\text{--}\text{C}_8$) homologues due to evaporation (Fig. 3a). In contrast, the Maui-1 oil displays a smooth and more substantial loss of short-chain *n*-alkanes up to $n\text{C}_{15}$, probably as a result of poor sample handling at some point since the oil was first discovered and sampled in 1969. This artificial loss of short to medium chain length *n*-

351 alkanes is not expected to have affected Re and Os because they largely reside within
352 the asphaltene fraction.

353 In contrast, the loss of *n*-alkanes in the Maari-MR8A and Manaia-2 oils is more
354 irregular and extends up to at least nC_{25} (Fig. 3a). This pattern of loss of *n*-alkanes,
355 commencing in the short- to medium-chain *n*-alkanes and then extending to long-chain
356 *n*-alkanes, is typical of biodegradation (Peters et al., 2005). Cross-plots comparing the
357 concentrations of nC_8 and nC_{14} to less easily biodegraded cyclic and branched
358 (isoprenoid) hydrocarbons of similar boiling points (Fig. 4) confirm these samples are
359 biodegraded to levels 2–3 of Peters et al. (2005). These Maari-Manaia oils are from
360 the shallower Moki Formation B sands, with reservoir temperatures of 50–52°C (Sykes
361 et al., 2011), conducive for biodegradation, whereas the remaining Family 11 oils are
362 from the F and D sands with reservoir temperatures of c. 112–125°C (Sykes et al.,
363 2011), well beyond the upper temperature limit of 60–80°C for significant
364 biodegradation (Peters et al., 2005). The apparent slight biodegradation of the Maui-1
365 oil indicated in Figure 3a is more likely an artefact of the significant loss of short-chain
366 *n*-alkanes experienced by this sample (Fig. 3a).

367 Although the Tui and Maui oils are not biodegraded, they are variably water-washed,
368 as are the biodegraded Maari-Manaia oils. This is indicated by their preferential loss
369 of the more water-soluble aromatic hydrocarbons compared to branched and cyclic
370 hydrocarbons of similar boiling point. Cross-plots comparing relative concentrations of
371 C_6 – C_8 cyclic and branched hydrocarbons to aromatic hydrocarbons (Fig. 5a) and
372 benzene and toluene to nC_6 and nC_7 , respectively (Fig. 5b), show largely consistent
373 relative levels of water washing using the two sets of parameters. The Maui-1 sample
374 appears to have spurious results due to its large loss of short-chain *n*-alkanes (Fig.
375 3a). Amongst the other terrestrial oils, the Maui B and all of the Tui Area oils appear

376 more water-washed than the Maari-MR8A oil, despite not being biodegraded. The thin
377 (10–12 m) oil columns in the Pateke, Amokura and Tui pools overlie a strong aquifer
378 (NZOP, 2005), and the relative levels of water washing indicated by the loss of
379 aromatic hydrocarbons (Pateke>Amokura>Tui) match the present-day direction of
380 hydrodynamic flow between the fields, from Pateke to Tui.

381 Amongst the marine oil samples, the Kora-1(A) and Waitangi Seep samples have both
382 experienced significant loss of short-chain *n*-alkanes up to about C₁₅–C₁₆ (Fig. 3b).
383 This will likely have affected the parameters on which the assessments of
384 biodegradation (Fig. 4) and water washing (Fig. 5) are based. The Kora-1(A) oil is
385 unlikely to be biodegraded given that it is from a depth of 3128–3182 m within the
386 Tangaroa Formation with temperatures of approximately 110 °C (Kroeger et al., 2022).
387 In contrast, there is negligible loss of short-chain *n*-alkanes in the Kora-1(B) oil from
388 the Mohakatino Formation reservoir (Fig. 3b). This oil lies just within the indicated
389 fields of biodegradation in Figure 4, but as the reservoir temperature is 68°C (Sykes
390 et al., 2011), any biodegradation is likely to be minimal. This sample also appears to
391 be amongst the least water-washed of the oil samples (Fig. 5). Lastly, the Kaikoura
392 Seep oil is the most biodegraded of the oil samples, with almost all of the *n*-alkanes
393 having been lost (Fig. 3b), indicating biodegradation to level 3 (Fig. 4b).

394 **3.2. Source rock samples**

395 Samples representative of potential or similar source rocks that generated the oils
396 studied here (Rakopi, North Cape, Waipawa and Whangai formations) have previously
397 been analysed for Re and Os concentrations and isotopic compositions (summarised
398 in Table S1; Rotich et al., 2020; 2021). The samples from Rakopi and North Cape
399 formations comprise coals and a coaly mudstone, ranging in TOC from 12.9 to 68.4
400 wt.% and HI from 183 to 350 mg HC/g TOC (Table S1). These samples were originally

401 collected from various outcrops in the Collingwood district of northwest Nelson (Fig.
402 1). The marine source rock samples from the Waipawa and Whangai formations are
403 all mudstones. The Waipawa mudstones are significantly richer in TOC (1.7–9.7 wt.%)
404 and contain higher quality organic matter (HI 164–375 mg HC/g TOC) than those from
405 the Whangai Formation (TOC 0.84–1.08 wt.%, HI 112–232 mg HC/g TOC; Table S1).
406 These samples were obtained from a drill core from well Orui-1A in the Wairarapa
407 region (Fig. 1) and several outcrop locations (Taylor White section, Angora Road and
408 Blacks Quarry) in the southern Hawke’s Bay and Northland regions of North Island
409 (Fig. 1).

410 **3.3. Methods**

411 **3.3.1. Asphaltene precipitation**

412 The asphaltene fraction contains the majority of Re and Os in crude oil, and in most
413 cases possesses Re-Os isotopic compositions that are representative of the whole oil
414 (Selby et al., 2007; Georgiev et al., 2016; DiMarzio et al., 2018; Liu et al., 2019).
415 Separation of this fraction therefore pre-concentrates these elements and allows for
416 more precise Re and Os analyses to be undertaken. This is especially important for
417 New Zealand coal-sourced oils, given their typically very low asphaltene contents
418 (Sykes and Zink, 2018).

419 Asphaltenes precipitation from the bulk oil samples was carried out at GNS Science’s
420 Organic Geochemistry Laboratory using methods reported in Speight (2004) and
421 Selby et al. (2007). Stock oils were thoroughly mixed to remove heterogeneities
422 caused by density segregation during storage. Many of the coal-sourced crude oils
423 from New Zealand are solid at room temperature due to their medium to very high wax
424 contents. Therefore, the first step in the separation process involved heating the solid
425 stock oils to about 50°C to obtain a viscous liquid that was thoroughly mixed prior to

426 sub-sampling. The subsamples (~1 g) were placed in pre-heated glass vials where an
427 excess of *n*-heptane (40 ml) was added and thoroughly mixed before continuous,
428 gentle agitation overnight (at least 12 h) at room temperature using an orbital shaker.
429 The contents of the vials were then centrifuged at 3500 rpm for 10–15 min to allow
430 complete separation of precipitated asphaltene and soluble maltene fractions. Maltene
431 fractions were decanted to waste while the remaining residues (asphaltene fractions)
432 were transferred into pre-weighed glass vials and dried overnight on a hot plate at
433 60°C. Depending on asphaltene content, the above steps were repeated 2 to 30 times
434 per sample to obtain the required amount of asphaltene (~250 mg) for Re-Os analysis.

435 **3.3.2. Re-Os analysis**

436 Rhenium and Os analyses of the asphaltene fraction of the oil samples were
437 undertaken at Durham University's laboratory for Source Rock and Sulfide
438 Geochronology and Geochemistry in 2018 following previously published protocols
439 (e.g., Selby et al., 2007; Liu et al., 2019). In brief, asphaltene fractions (150–200 mg)
440 were transferred into Carius tubes using small amounts of chloroform (CHCl₃; ≤1 ml)
441 and dried on a hot plate at 60°C overnight to evaporate the CHCl₃. After complete
442 solvent removal, a known amount of ¹⁹⁰Os and ¹⁸⁵Re mixed tracer solution and inverse
443 *aqua-regia* digestion mixture (3 ml 12 N HCl + 6 ml 15.5 N HNO₃) were sequentially
444 added, the tube sealed and then placed in an oven at 220°C for 24 h. The Os fraction
445 was extracted and purified from the inverse *aqua-regia* solution using solvent
446 extraction (CHCl₃ and back extraction in HBr) and micro-distillation methods,
447 respectively, whereas the Re fraction was extracted using anion exchange
448 chromatography (HCl-HNO₃). The obtained Re and Os fractions were then loaded
449 onto nickel and platinum wire filaments, respectively, and their isotopic compositions
450 measured on the Thermo Scientific TRITON negative thermal ionisation mass

451 spectrometer (N-TIMS; Creaser et al., 1991) housed at the Arthur Holmes Laboratory,
452 Durham University. The total procedural blanks over the course of this study were 2.41
453 ± 0.07 pg Re and 0.12 ± 0.05 pg Os, with an average $^{187}\text{Os}/^{188}\text{Os}$ of 0.26 ± 0.01 (2
454 SD, $n = 4$). The average $^{185}\text{Re}/^{187}\text{Re}$ value for the Re standard solution was $0.5989 \pm$
455 0.0016 (2 SD, $n = 10$), which is in excellent agreement with previously published data
456 (e.g., Cumming et al., 2014; Liu et al., 2019). The average $^{187}\text{Os}/^{188}\text{Os}$ value for the
457 in-house Durham Romil Osmium Standard (DROsS) was 0.16084 ± 0.00043 (2 SD, n
458 $= 8$), consistent with previously published data from other laboratories
459 (0.16078 ± 0.00024 , Liu and Pearson, 2014; 0.16091 ± 0.00015 , van Acken et al.,
460 2019). The uncertainties reported here include those from asphaltene weighing, blank
461 elemental and isotopic compositions, spike calibration, and the precision of the
462 repeated standard measurements.

463 Rhenium and Os analysis of the source rock samples were undertaken on powdered
464 aliquots of the whole rock material at the same time and at the same laboratory as the
465 oils (Rotich et al. 2020; 2021). Rhenium and Os concentrations are quoted with
466 respect to the whole rock, whereas the Re and Os concentrations of the oils are with
467 respect to the asphaltene fraction.

468 **4. Results**

469 Twelve of the 13 oil samples have low asphaltene contents, ranging from 0.9 to 2.4
470 wt.% (Table 1). In contrast, the asphaltene content of the Kaikoura Seep oil is higher
471 (15.5%), which is attributed to its more advanced degree of biodegradation, enriching
472 the asphaltene fraction through the loss of *n*-alkanes and other hydrocarbons. For all
473 oil samples, there is no significant direct relationship between asphaltene content and
474 Re and Os concentrations present in the asphaltene fractions (Fig. 6a, b), which range
475 from 0.18 to 5.90 ppb Re, 3.4 to 400.2 ppt Os and 1.3 to 149.9 ppt ^{192}Os (Table 1),

476 the latter being a measure of Os concentration unaffected by the radiogenic ingrowth
477 of ^{187}Os . Rhenium and ^{192}Os concentrations in the terrestrial Family 11 oils range from
478 0.18 to 0.45 ppb and 1.3 to 12.7 ppt (Fig. 7a), respectively, mirroring the low
479 concentrations of these elements in their potential Rakopi and North Cape Formation
480 coaly source rocks (0.19–0.37 ppb Re and 5.3–9.6 ppt ^{192}Os ; Fig. 7b, Table S1). The
481 low Re and Os concentrations in these terrestrial oils, coupled with their low
482 asphaltene contents, made precise Re and Os measurements difficult, with blank
483 corrections ranging from 3.8 to 10.5% for Re and 1.2 to 21.1% for Os. In contrast, the
484 asphaltene fractions of the marine oils (families 41 and 42) contain significantly higher
485 concentrations of both Re (0.91–5.90 ppb) and ^{192}Os (14.1–149.9 ppt; Fig. 7a),
486 mirroring, again, the higher concentrations of these elements in the marine mudstones
487 of the Waipawa and Whangai formations (3.6–62.3 ppb Re and 55.4–228.2 ppt ^{192}Os ;
488 Fig. 7b).

489 The Re and ^{192}Os concentrations in the asphaltene fraction of the oils are strongly
490 correlated ($R^2=0.93$) across the full set of 13 oils (Fig. 7a), with generally much higher
491 concentrations of both elements in the marine-sourced oils. The Re and ^{192}Os
492 concentrations in the terrestrial (coaly) and marine source rocks also show a strong
493 correlation ($R^2=0.91$) across the full sample set, with the marine source rocks having
494 greater concentrations than the terrestrial rocks (Fig. 7b). This is especially true for the
495 Waipawa Formation mudstones, which have consistently higher concentrations of Re
496 and ^{192}Os than the Whangai Formation mudstones. This suggests that the
497 enrichments of both elements are closely related in both the oils and the source rocks.

498 The asphaltene fractions of the Family 11 oils have $^{187}\text{Re}/^{188}\text{Os}$ ratios ranging from
499 31.1 to 306.0 and $^{187}\text{Os}/^{188}\text{Os}$ ratios from 0.514 to 1.164 (Table 1). These ratios show
500 no recognisable linear trend on an isochron diagram (Fig. 8). Within this oil family, the

501 Tui Area oils exhibit higher (i.e., more radiogenic) $^{187}\text{Os}/^{188}\text{Os}$ ratios (0.854–1.164) and
502 a smaller range in $^{187}\text{Re}/^{188}\text{Os}$ ratios (108.6–135.7) compared to those collected from
503 the Maui and Maari-Manaia fields ($^{187}\text{Os}/^{188}\text{Os}$ 0.514–0.681 and $^{187}\text{Re}/^{188}\text{Os}$ 31.1–
504 306.0; Table 1, Fig. 8). The $^{187}\text{Os}/^{188}\text{Os}$ and $^{187}\text{Re}/^{188}\text{Os}$ values for the asphaltene
505 fraction of the marine oils from families 41 and 42 range from 0.693 to 0.907 and 78.3
506 to 208.9, respectively (Table 1).

507 **5. Discussion**

508 **5.1. Evaluation of Re and Os geochronology of terrestrial oils**

509 The Family 11 oils were analysed to assess whether Re-Os geochronology can be
510 applied to terrestrial oils from Taranaki Basin. However, $^{187}\text{Re}/^{188}\text{Os}$ and $^{187}\text{Os}/^{188}\text{Os}$
511 ratios for these nine oils do not display any linear relationship on an isochron diagram
512 (Fig. 8), thus precluding a reliable Re-Os isochron date for this collection of terrestrial
513 oils.

514 Studies have suggested that the processes of oil generation and migration lead to
515 homogenisation of $^{187}\text{Os}/^{188}\text{Os}$ ratios and development of a Re-Os isochron in crude
516 oils (e.g., Selby and Creaser, 2005; Lillis and Selby, 2013; Liu et al., 2018). For
517 example, Re-Os data obtained from oil sand deposits of Alberta, Canada, yield an age
518 of 111.6 ± 5.3 Ma, which is in agreement with burial history models predicting
519 petroleum generation and migration at 110 Ma (Selby and Creaser, 2005). Similarly,
520 Re-Os dates for bitumen from the Polaris Mississippi Valley-type Zn–Pb deposit (Selby
521 et al., 2005) coincide with Rb–Sr sphalerite and paleomagnetic ages for the
522 mineralization of the Polaris deposit suggesting that the Re-Os isotope systematics
523 record the timing of bitumen migration. Lillis and Selby (2013) also presented Re-Os
524 data for crude oils from the Phosphoria petroleum system that yield an age of $211 \pm$
525 21 Ma consistent with the timing of oil generation and migration. Rhenium-osmium

526 isotope data for crude oils from the Duvernay petroleum system in Canada yield an
527 age of 66 ± 31 Ma, which is consistent with basin modelling derived timing of
528 hydrocarbon generation from the Duvernay Formation (Liu et al., 2018). If generation
529 and migration are the only processes needed for development of an oil isochron, then
530 the lack of a linear relationship for the Family 11 oils suggests that: (1) there was
531 insufficient homogenisation of the oils generated from coaly source rock intervals with
532 widely variable initial $^{187}\text{Os}/^{188}\text{Os}$ (Os_i) values and Re abundance, the latter resulting
533 in heterogeneous $^{187}\text{Os}/^{188}\text{Os}$ values over time as the ^{187}Re decays, (2) there is an
534 insufficient spread in $^{187}\text{Re}/^{188}\text{Os}$ values, (3) the Re-Os isotope systematics of the oils
535 were subsequently disturbed, and/or (4) there has been insufficient time since
536 homogenisation for the evolution of an isochron. It should be noted that wide scatter
537 on Re-Os isochron diagrams is not restricted to terrestrial oils, having previously been
538 documented in oils from marine and lacustrine systems (e.g., Cumming et al., 2014;
539 Liu et al., 2018).

540 Various scenarios have been proposed for charging of the Tui Area, Maui and Maari-
541 Manaia fields, with potential Late Cretaceous terrestrial kitchens including the Maui
542 and Pihama sub-basins, the Kahurangi Trough and a local Maari sub-basin beneath
543 the Maari structure (Fig. 2; Funnell et al., 2001; 2004; Matthews, 2002; 2008; Kroeger
544 et al., 2016; 2021; Reilly et al., 2016; Smith et al., 2016; Seebeck et al., 2019). The
545 more recent basin modelling studies favour charging of the Tui Area Field from the
546 northern Kahurangi Trough; the Maui Field, primarily from the Maui sub-basin, with
547 migration across the Cape Egmont Fault Zone; and the Maari-Manaia Field primarily
548 from the Maui sub-basin, potentially with a subordinate local fluid contribution from the
549 small Maari sub-basin (Fig. 2; Smith et al., 2016; Kroeger et al., 2016, 2021; Seebeck
550 et al., 2019). In all cases, the abundance of gymnosperm-derived diterpene
551 biomarkers within the oils indicates derivation from Late Cretaceous coaly rocks of the

552 Rakopi and North Cape formations (Killops et al., 1994; Sykes et al., 2012; Sykes and
553 Zink, 2018; Sykes, 2019). These formations have a maximum combined thickness of
554 up to ~2700 m (Seebeck et al., 2019) and their coaly rocks display considerable
555 variation in initial $^{187}\text{Os}/^{188}\text{Os}$ (Os_i) values and Re abundance. While the full range of
556 Os_i values for these formations is unknown, calculated values for eight coaly rock
557 samples analysed are 0.82–1.24 for Rakopi Formation (at 78 Ma) and 0.31–0.46 for
558 the younger North Cape Formation (at 67 Ma) (Rotich et al., 2021). The difference
559 between the two formations is attributed primarily to changing contributions of Os from
560 weathering of upper continental crust (Rakopi Formation) and freshly erupted mafic
561 rocks (North Cape Formation) (Table S1; Rotich et al., 2021). Rhenium abundances
562 for the above eight coaly rock samples are low, varying from 0.19 to 0.37 (Table S1).
563 However, as the source kitchens for the Tui Area, Maui and Maari-Manaia oils are on
564 the order of 50 km apart and several hundred meter-intervals of coaly source rocks
565 can lie within the oil window at any given time, it is highly likely that the expelled oils
566 would have varied widely in Re abundance and initial Os isotope compositions. It is,
567 therefore, not entirely unexpected to see such scatter in $^{187}\text{Os}/^{188}\text{Os}$ values on the
568 isochron diagram (Fig. 8), especially given that the nine oils were likely generated from
569 different coal measure intervals in two separate depocentres (i.e., northern Kahurangi
570 Trough and Maui sub-basin).

571 Notably, even the five Tui Area oils display significant variation in $^{187}\text{Os}/^{188}\text{Os}$ values
572 (0.85–1.16, Table 1), despite being from a single spill-fill chain that links the Tui,
573 Amokura and Pateke accumulations. Either these accumulations were filled from
574 separate, sequential charges of oil from different source rock intervals of the Rakopi
575 Formation, with incomplete homogenisation of $^{187}\text{Os}/^{188}\text{Os}$ compositions through
576 migration and accumulation, or the Os isotope compositions were subsequently
577 disturbed within the reservoir.

578 One reason for selecting the nine Family 11 oil samples from different fields was to
579 maximise the likelihood of achieving a sufficient spread in $^{187}\text{Re}/^{188}\text{Os}$ ratios (Fig. 2;
580 Selby and Creaser, 2005). The obtained $^{187}\text{Re}/^{188}\text{Os}$ values for the asphaltene
581 fractions of these oils, however, vary by only 275 units, which is low when compared
582 to most oils successfully dated using the Re-Os geochronometer (up to 1500 units;
583 e.g., Selby and Creaser, 2005; Selby et al., 2005; Finlay et al., 2011; Lillis and Selby,
584 2013; Cumming et al., 2014; Liu et al., 2018). Asphaltenes obtained from southern
585 Australian asphaltites have produced reliable Re-Os oil isochrons with a much lower
586 spread in $^{187}\text{Re}/^{188}\text{Os}$ ratios (~147 units) than the Family 11 oils (Corrick et al., 2019;
587 Scarlett et al., 2019). However, as the asphaltites from that study were generated in
588 the mid-Cretaceous (104 ± 12 Ma; Corrick et al., 2019; Scarlett et al., 2019), they
589 would have radiogenically evolved more to better define an isochron compared to the
590 Family 11 oils, which, as discussed below, only commenced expelling significant oil
591 since the Late Miocene (Kroeger et al., 2016; 2021). Indeed, when the Re-Os isotope
592 data for the Maui and Maari-Manaia oils are forward modelled to, for example, 100 Ma
593 in the future, a good correlation is obtained (Table 1). Not so for the Tui Area oils as
594 high variation in Os_i values and a small range in $^{187}\text{Re}/^{188}\text{Os}$ values hinder any
595 correlation. We therefore consider that the lack of an isochron fit for the Family 11 oils
596 is largely due to a combination of high variation in Os_i values inherited from different
597 Late Cretaceous coaly source rock intervals, an insufficient spread in $^{187}\text{Re}/^{188}\text{Os}$
598 values, and insufficient time since oil expulsion for the evolution of an isochron,
599 although other factors discussed below may have also contributed.

600 Another potential cause of data point scatter on crude oil Re-Os isochron diagrams is
601 disturbance of the Re-Os systematics within the reservoir through processes such as
602 thermochemical sulfate reduction (TSR; Lillis and Selby, 2013), biodegradation and
603 water washing. TSR is a redox reaction that occurs in reservoirs containing anhydrite

604 or another source of sulfate, whereby petroleum is oxidized to carbon dioxide and
605 sulfate is reduced to hydrogen sulfide (Goldstein and Aizenshtat, 1994; Walters et al.,
606 2015). There is, however, no evidence of TSR having affected the Family 11 oils,
607 which show no detectable H₂S and only low CO₂ in bottom hole and separator PVT
608 samples (Sykes et al., 2011). Similarly, of the nine Family 11 oils, only the two Maari-
609 Manaia oil samples (Maari-MR8A and Manaia-2) are biodegraded, but only to levels
610 2–3 (Section 3.1.2). The ¹⁸⁷Os/¹⁸⁸Os values of these two oils do not stand out from
611 those of the other Family 11 oils, and their ¹⁸⁷Re/¹⁸⁸Os values are only slightly higher.
612 Biodegradation to levels 2–3 is likely restricted to hydrocarbons in the maltene fraction,
613 sparing the more resistant asphaltene fraction within which much of the Re and Os
614 resides. Biodegradation can therefore also be discounted as a significant process
615 affecting the Re-Os systematics of these oils, consistent with the findings of other
616 studies of biodegraded oils and tar sands (Selby and Creaser, 2005; Finlay et al.,
617 2011; Lillis and Selby, 2013).

618 Contact experiments have demonstrated that Re and Os can readily transfer between
619 aqueous solutions and oils (Mahdaoui et al., 2015; Hurtig et al., 2019), and all of the
620 Tui Area, Maui and Maari-Manaia oils in this study appear to have been water-washed
621 to varying degrees (Fig. 5). The Re-Os systematics of these low Re- and Os-bearing
622 oils may be more vulnerable to the adverse effects of water washing because water-
623 oil ratios of less than 100 (based on estimated concentration levels of 4 ppt Re and
624 0.07 ppt Os in groundwaters) would be required to completely overprint their Re-Os
625 systematics (e.g., Colodner et al., 1993; Paul et al., 2010; Mahdaoui et al., 2015). Such
626 water-oil ratios are likely in conventional petroleum systems, such as in offshore
627 Taranaki Basin, because reservoir rocks are commonly fully saturated with formation
628 water prior to the ingress of oil (Magoon and Dow, 1994; Levorsen, 2001). Moreover,
629 in the case of the Tui Area oils, the three pools of oil overlie an aquifer with a strong

630 bottom water drive (NZOP, 2005; Matthews et al., 2008), which would help sustain Re
631 and Os concentration and isotope ratio gradients across the oil-water interface. The
632 relative degree of water washing indicated between the three oil pools
633 (Pateke>Amokura>Tui) matches the present-day direction of hydrodynamic flow from
634 Pateke to Tui, and would account for the consistent difference in $^{187}\text{Os}/^{188}\text{Os}$ ratios
635 between the four Pateke and Tui oils if the $^{187}\text{Os}/^{188}\text{Os}$ composition of the formation
636 water is approximately 0.8 or lower (Fig. 8). However, there are currently no Os isotope
637 data for formation water in Taranaki Basin to support this assumption, and $^{187}\text{Os}/^{188}\text{Os}$
638 values for formation waters elsewhere are generally more radiogenic (>1; Paul et al.,
639 2010; Hnatyshin, 2018). Furthermore, it has been shown that formation waters in deep
640 subsurface aquifers are generally severely depleted in Re and Os (Hnatyshin, 2018),
641 and thus crude oils may not gain appreciable Re and Os from any interaction with
642 these waters. This is evident in crude oils from the Duvernay petroleum system in the
643 Western Canada Sedimentary Basin whose $^{187}\text{Os}/^{188}\text{Os}$ compositions are much lower
644 than estimated $^{187}\text{Os}/^{188}\text{Os}$ values for formation fluids in the basin, and thus, less likely
645 to have been impacted by interaction with these fluids (Liu et al., 2018). Therefore,
646 there is no definitive evidence to indicate whether any of the variation in $^{187}\text{Os}/^{188}\text{Os}$
647 ratios amongst the Tui Area oils or the other Family 11 oils can be attributed to water
648 washing, rather than incomplete homogenisation of highly variable initial $^{187}\text{Os}/^{188}\text{Os}$
649 values.

650 **5.2. Some comments on the actual event being dated**

651 The terrestrial oils in this study did not yield a Re-Os isochron. However, this does not
652 discount the possibility of isochrons being obtained for terrestrial oils elsewhere.
653 Should an isochron emerge, it is important to consider what actual event or process is
654 being dated—oil generation, migration or emplacement—particularly if the assigned

655 age is critical for establishing temporal relationships between elements of a petroleum
656 system. Most studies of marine and lacustrine oils have assigned isochron ages to the
657 time of oil generation (e.g., Cumming et al., 2014; Liu et al., 2018). However, the
658 process of oil generation is confined to the host kerogen generating the oil (Pepper
659 and Corvi, 1995a), thus the heterogeneity of source rock $^{187}\text{Os}/^{188}\text{Os}$ composition will
660 still exist within the generated oil residing within the source rock interval (Selby and
661 Creaser, 2005; Selby et al., 2007; Finlay et al., 2011; Rooney et al., 2012; Cumming
662 et al., 2014; Liu et al., 2018). Adequate homogenisation of $^{187}\text{Os}/^{188}\text{Os}$ ratios, which is
663 a requisite condition for forming a Re-Os isochron, can only occur with the mixing of
664 oil that results from expulsion, migration and accumulation. For the more oil-prone,
665 marine and lacustrine source rock organofacies, oil expulsion and primary migration
666 tend to be efficient and in geological terms, are thought to occur relatively soon after
667 the onset of generation (Pepper and Corvi, 1995a; Liu et al., 2018). Moreover,
668 secondary migration is also generally an efficient process (Pepper and Corvi, 1995b),
669 occurring over relatively short periods of geological time. Thus, for marine and
670 lacustrine oils, it may be satisfactory to equate Re-Os isochron ages with oil
671 generation, but it still remains that homogenisation will not commence until migration
672 proceeds upon expulsion.

673 The distinction between the timing of generation and migration is more critical for
674 terrestrial oils because coaly organofacies tend to be both more heterogeneous and
675 less efficient expellers of oil (Pepper and Corvi, 1995b). In coaly source rocks with oil
676 potential, there is typically a significant time lag between the onset of oil generation
677 and when the kerogen pore saturation threshold is reached to enable expulsion. The
678 lag duration will depend on, among other things, source rock quality (mainly HI) and
679 the burial and thermal histories, but can be 40 Myr or more (Pepper, 1991; Pepper
680 and Corvi, 1995b; Zhao and Cheng, 1998; Wilkins and George, 2002; Sykes et al.,

681 2014). This is consistent with generation and expulsion histories extracted from the
682 model of Kroeger et al. (2022) for the Maui sub-basin and the Kahurangi trough (Fig.
683 9). We therefore propose that Re-Os isochron ages for terrestrial oils date the onset
684 of expulsion (i.e., start of migration) and that for oil-source fingerprinting, oil Os_i values
685 for undisturbed systems should match the $^{187}Os/^{188}Os$ composition of the source rock
686 at the time of oil expulsion (Os_e), rather than generation (Os_g).

687 **5.3. Os isotope fingerprinting of Family 11 terrestrial oils**

688 Given that oil expulsion from the central Maui sub-basin and northern Kahurangi
689 Trough is modelled to have commenced only within approximately the last 13 to 3 Myr
690 (Fig. 9; Kroeger et al., 2016; 2021), we consider 10 Ma as the average oil expulsion
691 date for the purpose of calculating the Os_i and Os_e values from the present-day Re-
692 Os data for the oil and source rock samples, respectively. The use of an average oil
693 expulsion date does not affect the outcome of Os isotope fingerprinting because Os_i
694 and Os_e values will generally co-vary with changing oil expulsion dates, especially
695 when the $^{187}Re/^{188}Os$ values exhibited by both the terrestrial oils and source rocks are
696 low (≤ 306 for the samples studied here; Cumming et al., 2014).

697 The Os_i values for the Family 11 terrestrial oils collectively display a wide range from
698 0.47 to 1.14, with a mean value of 0.78 (Table 1; Fig. 10). Although these values
699 overlap much of the range of Os_e values (0.38–1.38, mean = 0.81) for their inferred
700 Late Cretaceous Rakopi and North Cape Formation source rocks (Table S1), they also
701 show considerable overlap with the Os_e values of Paleocene (Farewell Formation) and
702 Eocene (Mangahewa Formation) coaly rocks (Fig. 10). Moreover, they also overlap
703 the Os_i values for the Family 41 and 42 marine oils and their potential Waipawa and
704 Whangai source rocks, respectively. The Os_i values of the terrestrial oils in this study
705 are thus not sufficiently specific to provide a unique fingerprint of their Late Cretaceous

706 coaly source rock formations on their own. Osmium isotope compositions therefore
707 appear to have limited potential for broad oil-source rock correlation within the
708 predominantly coal-sourced petroleum systems of Taranaki Basin.

709 Within Family 11, the Tui Area oils exhibit notably higher (more radiogenic) Os_i values
710 (0.84–1.14) than oils from the Maui and Maari-Manaia fields, which have only
711 moderately radiogenic Os_i values (0.47–0.65). This difference is inferred to be a direct
712 result of generation from different Late Cretaceous coaly source rock intervals within
713 the northern Kahurangi Trough and Maui sub-basin, possibly with greater relative
714 contributions from the Rakopi and North Cape formations to the Tui Area and
715 Maui/Maari-Manaia oil fields, respectively (Fig. 10). Rakopi Formation coaly sediments
716 appear to have more radiogenic Os compositions, possibly reflecting greater input
717 from weathering of upper continental crust, whereas North Cape Formation coaly
718 sediments have less radiogenic Os compositions, possibly from weathering of freshly
719 erupted mafic rocks (Rotich et al., 2021). The most recent basin models identify
720 Rakopi Formation as the principal source rock unit in both the Maui sub-basin and
721 Kahurangi Trough based on coaly source rock distribution, volume and maturity
722 (Kroeger et al., 2016; 2021). However, the less radiogenic Os compositions of the oils
723 in the Maui and Maari-Manaia fields may reflect a greater, though still subordinate,
724 contribution from the North Cape Formation.

725 Whilst the difference in Os_i values between the Tui Area and the Maui and Maari-
726 Manaia oils may add further support for the derivation of these oils from different sub-
727 basins, it is evident from the wide variation in Os_i values amongst the Family 11 oils
728 that more oil and source rock Re-Os isotopic data are needed to better constrain the
729 underlying controls on the $^{187}Os/^{188}Os$ compositions of the terrestrial oils.

730

731 **5.4. Os isotope fingerprinting of Family 41 and 42 marine oils**

732 Wide variation in initial $^{187}\text{Os}/^{188}\text{Os}$ compositions is also reported to have hampered
733 petroleum geochronology and oil-source correlation in some lacustrine (Cumming et
734 al., 2014) and marine (Liu et al., 2018) petroleum systems. The marine oils of this
735 study provide a further example. The average age of 10 Ma used to calculate Os_i and
736 Os_e values for fingerprinting the Family 11 terrestrial oils and their source rocks is also
737 deemed appropriate for comparing the Family 41 and 42 marine oils and their potential
738 source rocks. Family 41 oils from the Kora Field (Fig. 1) are modelled to have been
739 expelled from the Late Paleocene Waipawa Formation from the Miocene (15 Ma) to
740 present day (Brett, 2005; Clayton, 2011; Kroeger et al., 2022). Similarly, thermal
741 maturity models from a number of sites in East Coast Basin indicate potential
742 generation and expulsion of Family 42 oils from the Whangai Formation from the
743 Miocene to Pliocene (Field et al., 1997; Schlumberger, 2017).

744 The calculated Os_i values at 10 Ma for the two Family 41 oils from Kora-1 are markedly
745 different (Fig. 10). The Kora-1(A) oil from the Eocene Tangaroa Formation sandstone
746 reservoir has a moderately radiogenic Os_i value (0.66), consistent with the calculated
747 Os_e values (0.48–0.68) for the Waipawa Formation source rock samples (Fig. 10). In
748 contrast, the Os_i value (0.90) for the Kora-1(B) oil from the Miocene Mohakatino
749 Formation volcanoclastic reservoir is significantly more radiogenic. Both oils have the
750 distinctive heavy carbon isotopic signature and high C_{30} sterane content that are
751 diagnostic of the Waipawa Formation, and were undoubtedly sourced from this unit
752 (Reed, 1992; Killops et al., 1994; Killops, 1996; Rogers et al., 1999; Sykes et al., 2012;
753 Naeher et al., 2019). As the Waipawa Formation is estimated to be <30 m thick in the
754 vicinity of Kora Field (Clayton, 2011), it is reasonable to assume that the entire
755 thickness of the formation would lie within the oil expulsion window at the same time,

756 thus leaving two possible scenarios to explain the high O_s value of the Kora-1(B) oil:
757 1) the Re-Os systematics of this oil have been disturbed, or 2) this oil was derived
758 from a different fetch or drainage area of the Waipawa Formation to that of the Kora-
759 1(A) oil. The latter is consistent with the modelling results of Kroeger et al. (2022)
760 which suggest that the Miocene Kora-1(B) accumulation was charged late, in the Plio-
761 Pleistocene and quite possibly from a fetch area further away from the volcano
762 unaffected by magmatic heating.

763 Disturbance of the Re-Os systematics through thermochemical sulfate reduction (Lillis
764 and Selby, 2013) can be discounted because the Kora-1(B) oil shows no detectable
765 H_2S or CO_2 in bottom hole PVT sample (Sykes et al., 2011). Any biodegradation in the
766 Kora-1(B) sample is also considered minimal (Fig. 4). Disturbance through interaction
767 with reservoir formation waters (Mahdaoui et al., 2015; Hurtig et al., 2019) seems
768 unlikely because most volcanic rocks have non-radiogenic $^{187}Os/^{188}Os$ compositions
769 (generally <0.3 ; e.g., Lassiter and Luhr, 2001; Suzuki and Tatsumi, 2006), whereas
770 the Kora-1(B) oil, reservoired in volcanoclastic rocks, has a distinctly more radiogenic
771 O_s value (0.90) than the Kora-1(A) oil (0.66).

772 No Waipawa Formation mudstone samples of sufficient size for Re and Os isotope
773 analysis are available from the immediate vicinity of Kora Field. However, in their study
774 of the Re-Os systematics of Waipawa Formation in East Coast Basin (Fig. 1), Rotich
775 et al. (2020) suggested that scatter in $^{187}Os/^{188}Os$ values within the Taylor White
776 section may have been caused by localised variation in seawater O_s values related
777 to the episodic and localised influx of large amounts of terrestrial organic matter
778 (Naeher et al., 2019). Such influxes may have supplied high loads of continental-
779 derived Os with more radiogenic $^{187}Os/^{188}Os$ compositions, not only within the Taylor
780 White section but also, potentially, within the respective fetch areas for the Kora-1(A)

781 and (B) oils. Without further data, however, the cause of the higher Os_i value of the
782 Kora-1(B) oil compared to those of the Kora-1(A) oil and Waipawa mudstone samples,
783 remains uncertain.

784 Similarly, the underlying cause of the higher Os_i values of the Family 42 Waitangi
785 (0.78) and Kaikoura (0.86) seep oils compared to the Os_e values of the potential
786 Whangai Formation source rock (0.46–0.58; Fig. 10) remains unknown. The Os_e
787 values are from the upper (Paleocene) section of the Whangai Formation, which could
788 possibly explain the less radiogenic values given that seawater $^{187}Os/^{188}Os$
789 composition in the Paleocene ranged from 0.3 to 0.4 (Peucker-Ehrenbrink and
790 Ravizza, 2012). Deeper sections (Late Cretaceous) of the Whangai Formation would
791 likely exhibit more radiogenic Os_e values because Late Cretaceous seawater
792 $^{187}Os/^{188}Os$ composition ranged from 0.6 to 0.7 (Peucker-Ehrenbrink and Ravizza,
793 2012). However, these sections generally have very poor oil generation potential (Field
794 et al., 1997; Hollis and Manzano-Kareah, 2005). Therefore, the mismatch of
795 $^{187}Os/^{188}Os$ compositions lends further support to previous suggestions that the Family
796 42 seep oils are not derived from known organofacies of the Whangai Formation.
797 Rather, they are more likely to have originated from another Late Cretaceous marine
798 source unit with similar biomarker and carbon isotope compositions as the Whangai
799 Formation.

800 **6. Conclusions**

801 This is the first study of the Re-Os systematics of terrestrial (coal-sourced) oils.
802 Although a radiometric age could not be determined, the study nonetheless provides
803 useful insights into the potential application of Re-Os geochronology and Os isotope
804 fingerprinting in coal-sourced petroleum systems. Nine genetically related terrestrial
805 oils (Family 11) from offshore Taranaki Basin contain similar, low concentrations of Re

806 and ^{192}Os as their correlative Late Cretaceous coaly source rocks (Rakopi and North
807 Cape formations). The Re and ^{192}Os concentrations in these terrestrial oils are
808 generally one to two orders of magnitude lower than those in marine oils from Taranaki
809 (Family 41) and East Coast (Family 42) basins.

810 The $^{187}\text{Re}/^{188}\text{Os}$ and $^{187}\text{Os}/^{188}\text{Os}$ ratios of the Family 11 terrestrial oils do not display
811 a linear relationship and hence did not yield a Re-Os isochron age. We attribute this
812 to: (1) insufficient homogenisation of widely variable initial $^{187}\text{Os}/^{188}\text{Os}$ (Os_i) values and
813 Re abundance inherited from thick, coaly source rock intervals (up to about 2700 m)
814 within the Maui sub-basin and northern Kahurangi Trough kitchens; (2) insufficient
815 spread of $^{187}\text{Re}/^{188}\text{Os}$ values (only 275 units); (3) insufficient time since oil expulsion
816 for the evolution of an isochron (expulsion is modelled from approximately 10 Ma to
817 the present day); and (4) potentially, water washing of the oil columns. Although the
818 oil samples are all water-washed to varying degrees, there is no definitive evidence
819 that water washing has disturbed the Re-Os systematics. We recommend that future
820 Re-Os studies of terrestrial oils be done on simple, well-characterised systems with a
821 single source rock, relatively fast petroleum generation, well-defined migration
822 pathways and limited post-generation alterations.

823 Most previous studies of marine and lacustrine oils have assigned Re-Os isochron
824 ages to the time of oil generation. However, as adequate homogenisation of
825 $^{187}\text{Os}/^{188}\text{Os}$ ratios can only occur with the mixing of oil that results from expulsion,
826 migration and accumulation, isochron ages correspond best to the timing of oil
827 expulsion. This distinction between the timing of oil generation and migration is more
828 critical for terrestrial oils because of the typically longer time lag between the onset of
829 oil generation and expulsion from coaly source rocks, which, in the case of the Family
830 11 study oils, is modelled to be up to about 40 Myr. Longer lag times are possible in

831 other (sub-)basins, depending on, among other things, coaly source rock quality and
832 the burial and thermal histories. We therefore suggest that Re-Os isochron ages for
833 terrestrial oils should date the onset of expulsion (i.e., start of migration) and that for
834 oil-source correlation, calculated oil Os_i values should match the calculated
835 $^{187}Os/^{188}Os$ ratios of the source rock at the time of oil expulsion (Os_e), rather than
836 generation (Os_g).

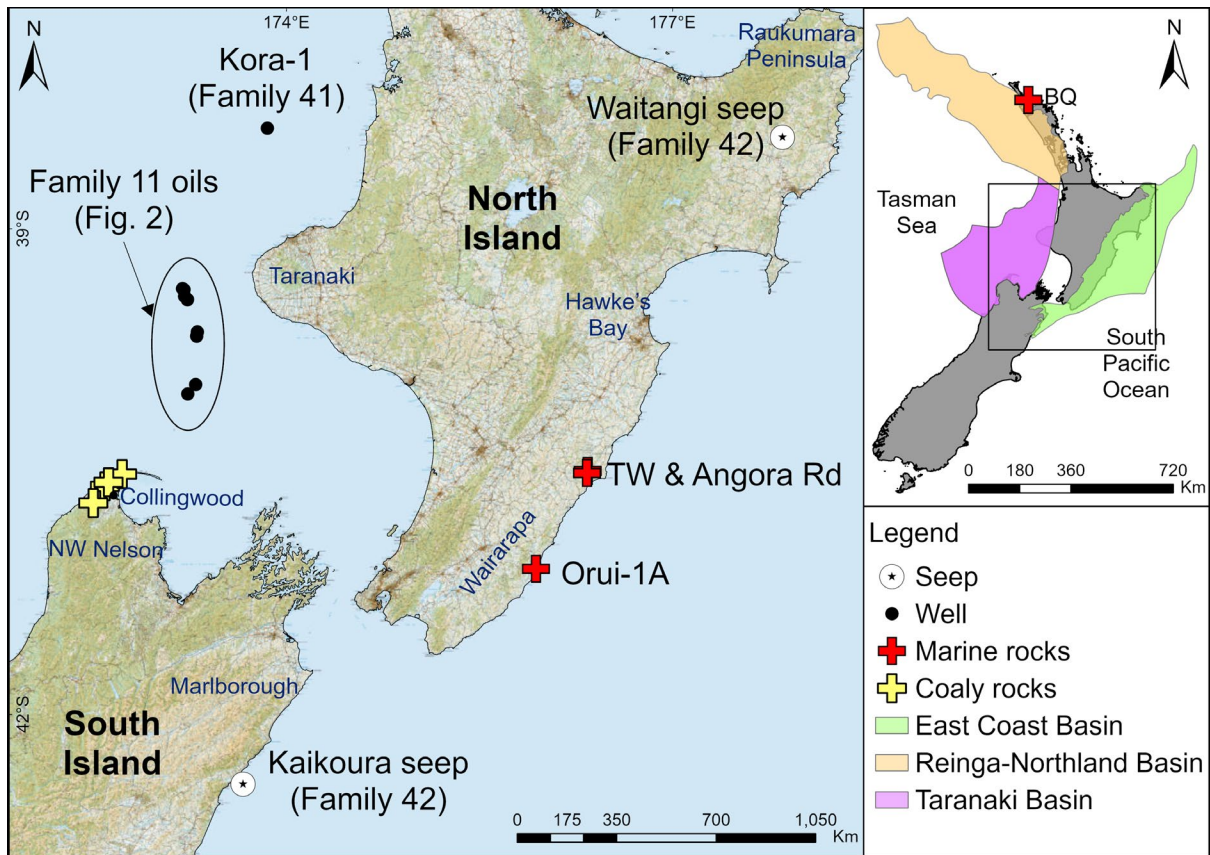
837 Calculated Os_i values for the Family 11 study oils display a wide range and do not
838 provide a unique fingerprint of their Late Cretaceous coaly source rock formations. Os
839 isotope compositions therefore appear to have limited potential for broad oil-source
840 rock correlation within the predominantly coal-sourced petroleum systems of Taranaki
841 Basin. Nonetheless, the observed Os_i values are distinct between two sub-basins
842 which, consistent with basin modelling, suggest charge of the Tui Area Field and the
843 Maui and Maari-Manaia fields from different source kitchens. Significantly higher
844 (more radiogenic) Os_i values of the Tui Area oils may indicate a charge predominantly
845 from the Rakopi Formation in the Kahurangi Trough, whilst the less radiogenic Os_i
846 values of the Maui and Maari-Manaia oils may suggest a greater contribution from the
847 North Cape Formation in the Maui sub-basin, although further samples are needed to
848 confirm this.

849 **Acknowledgements**

850 This study and the PhD scholarship awarded to EKR were primarily funded by the
851 Ministry of Business, Innovation and Employment (MBIE), New Zealand, as part of the
852 GNS Science-led research programme “Understanding petroleum source rocks,
853 fluids, and plumbing systems in New Zealand basins: a critical basis for future oil and
854 gas discoveries” (Contract C05X1507). We thank Antonia Hoffman, Geoff Nowell and
855 Chris Ottley of Durham University, Roger Tremain and Andy Phillips of GNS Science,

856 and Bruce Charlier and Luisa Ashworth of Victoria University of Wellington for their
857 technical assistance. Special thanks to all the staff at the National Core Store in
858 Featherston for providing access and assistance during oil sub-sampling. We thank
859 Katz Suzuki, Candace Martin and Warren Dickinson for feedback on an earlier version
860 of the manuscript. This contribution has benefited from thoughtful and constructive
861 comments of two anonymous reviewers, and the editorial handling of Professor
862 Quanyou Liu.

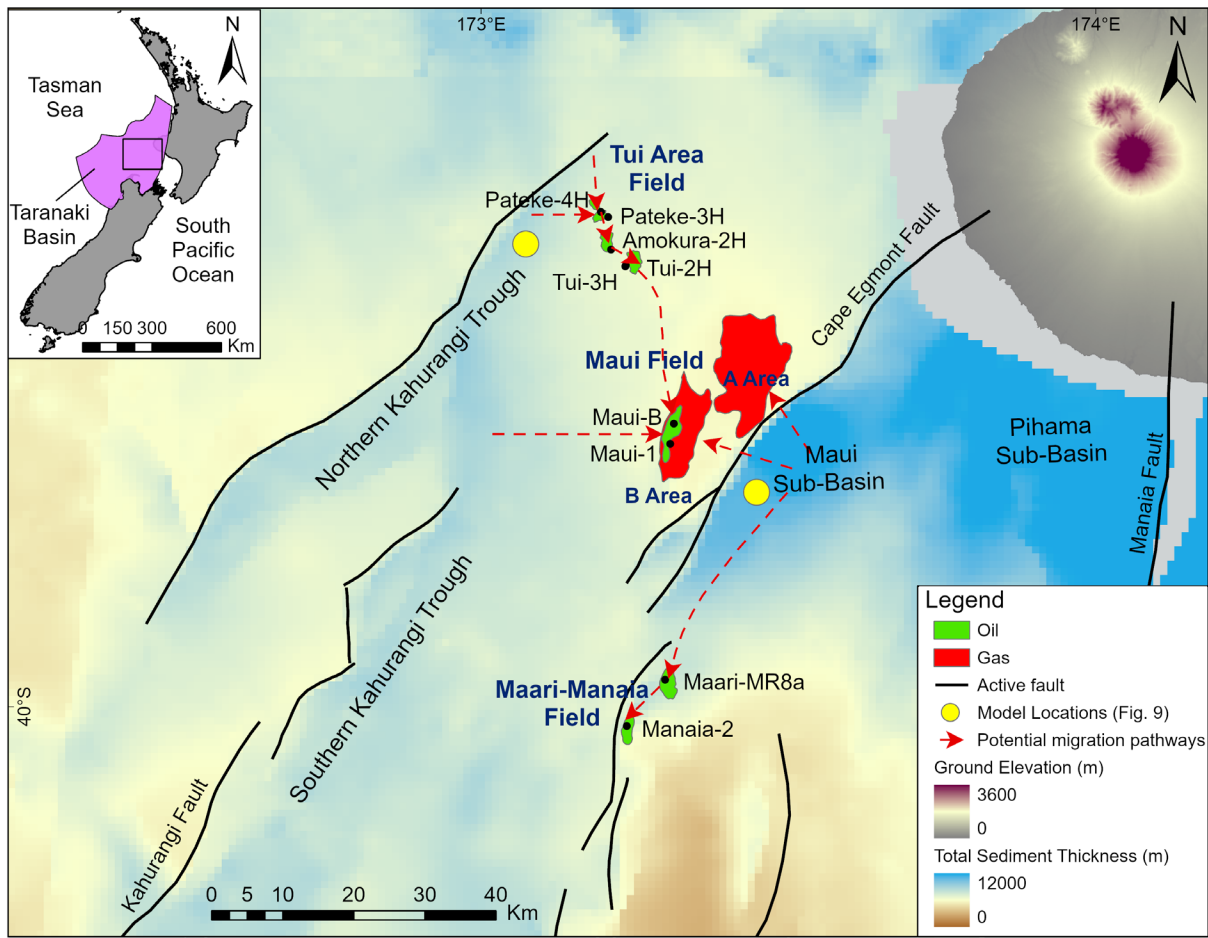
863



865

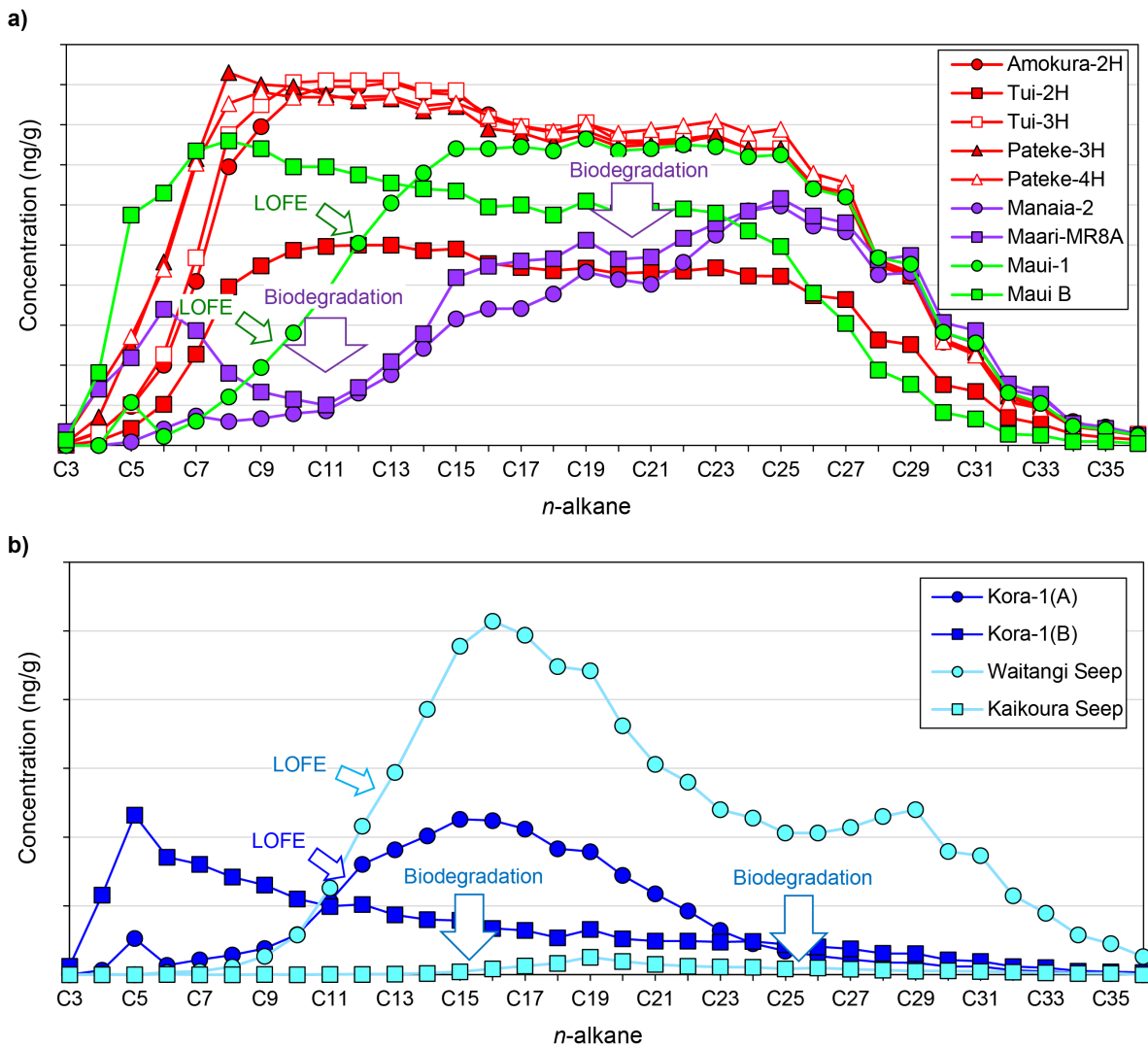
866 **Fig. 1.** Locality map of the studied oil and source rock samples in the Taranaki and
 867 East Coast basins and onshore Northland. TW = Taylor White outcrop; BQ = Blacks
 868 Quarry outcrop.

869



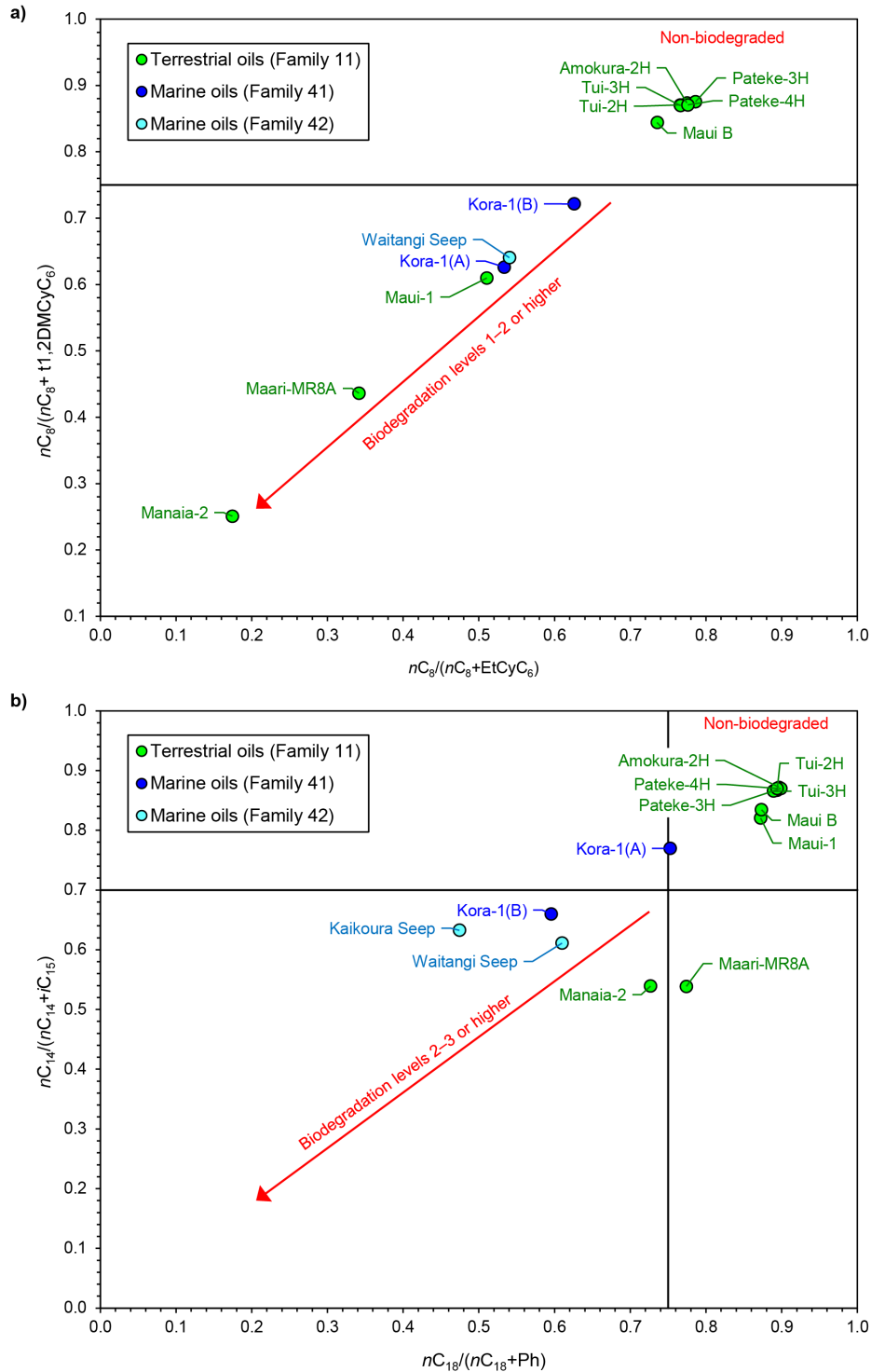
870

871 **Fig. 2.** Detailed map of Taranaki Basin showing distribution of the studied Family 11
 872 oils, oil and gas fields, potential migration pathways and major faults bounding Late
 873 Cretaceous sub-basins in which Rakopi and North Cape Formation coal measures are
 874 mapped (Matthews, 2008; Bull et al., 2016; Kroeger et al., 2016; 2021). The yellow
 875 dots mark the locations where oil and gas generation and expulsion histories in Figure
 876 9 were modelled.



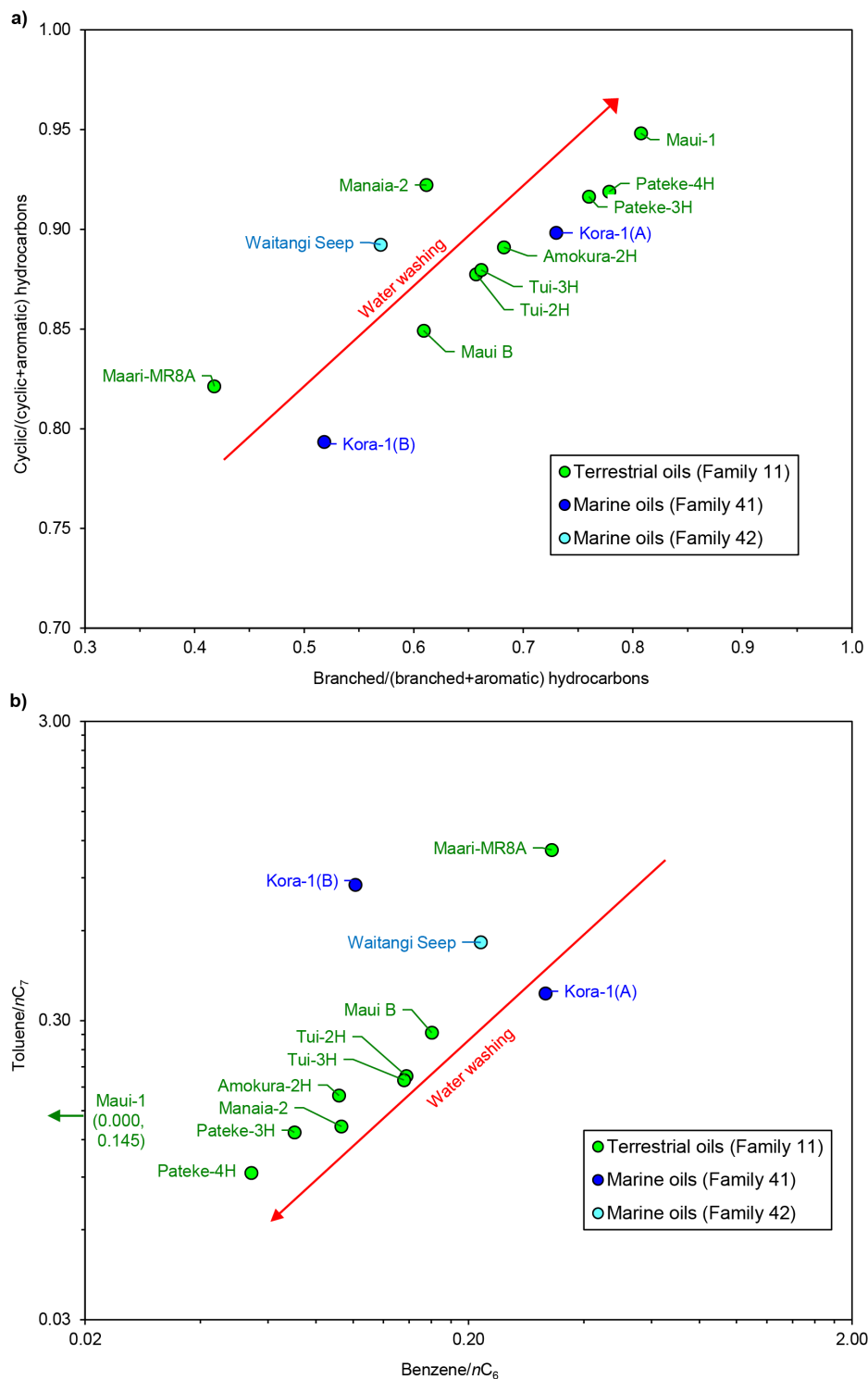
877

878 **Fig. 3.** *n*-alkane distributions of the (a) terrestrial and (b) marine study oils (data from
 879 Sykes and Zink, 2018; and GNS Science unpublished results). LOFE = loss of front-
 880 ends through evaporation.



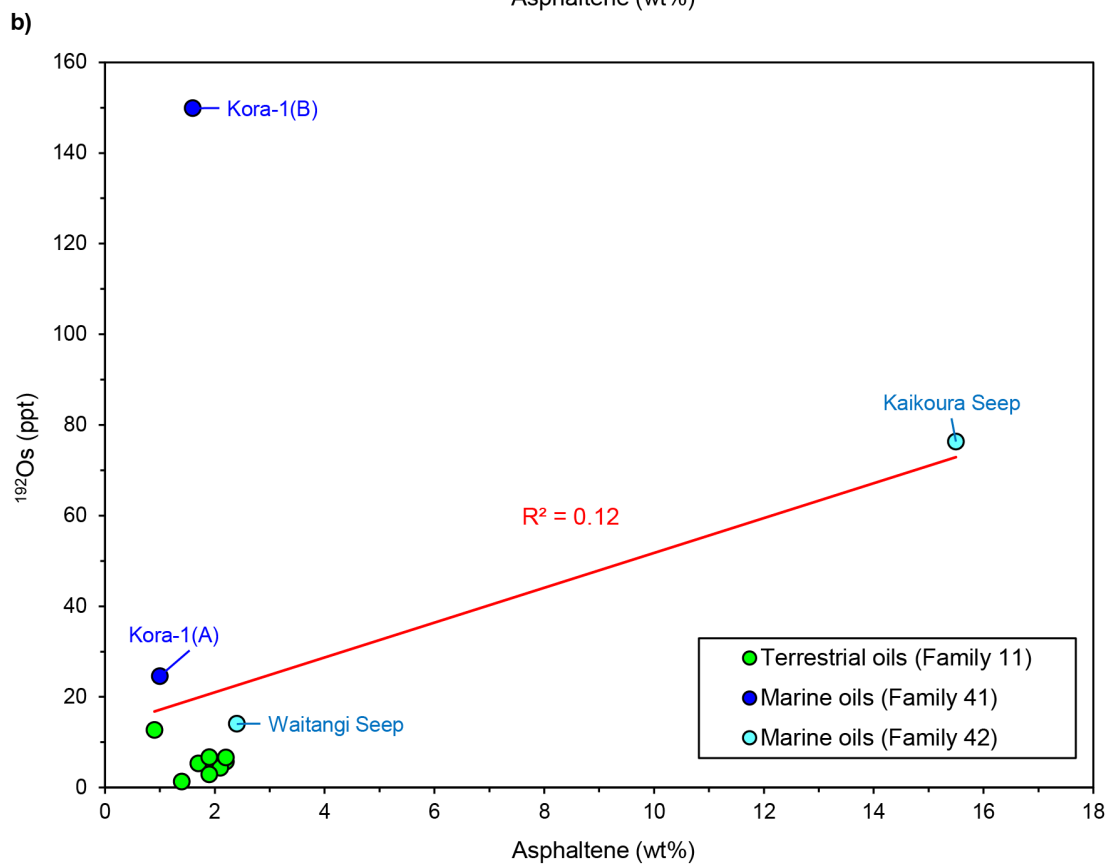
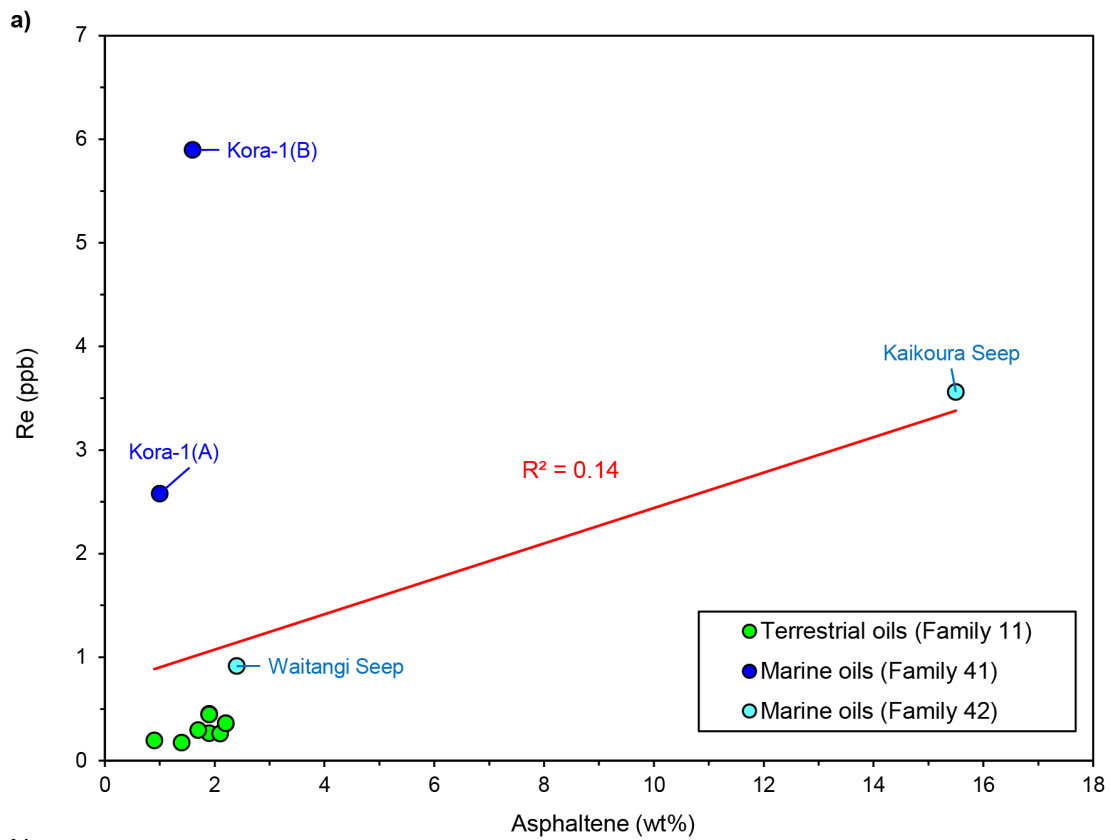
881

882 **Fig. 4.** Biodegradation of the terrestrial and marine study oils to (a) levels 1–2 or
 883 greater and (b) levels 2–3 or greater indicated by ratios of *n*-alkanes, cycloalkanes
 884 and isoprenoids. nC_8 : *n*-octane; *t*-1,2DMCyC₆: *trans*-1,2-dimethylcyclohexane;
 885 EtCyC₆: ethylcyclohexane; nC_{14} : *n*-tetradecane; nC_{18} : *n*-octadecane; *i*C₁₅: *iso*-
 886 pentadecane; Ph: phytane. Biodegradation levels are those of Peters et al. (2005).



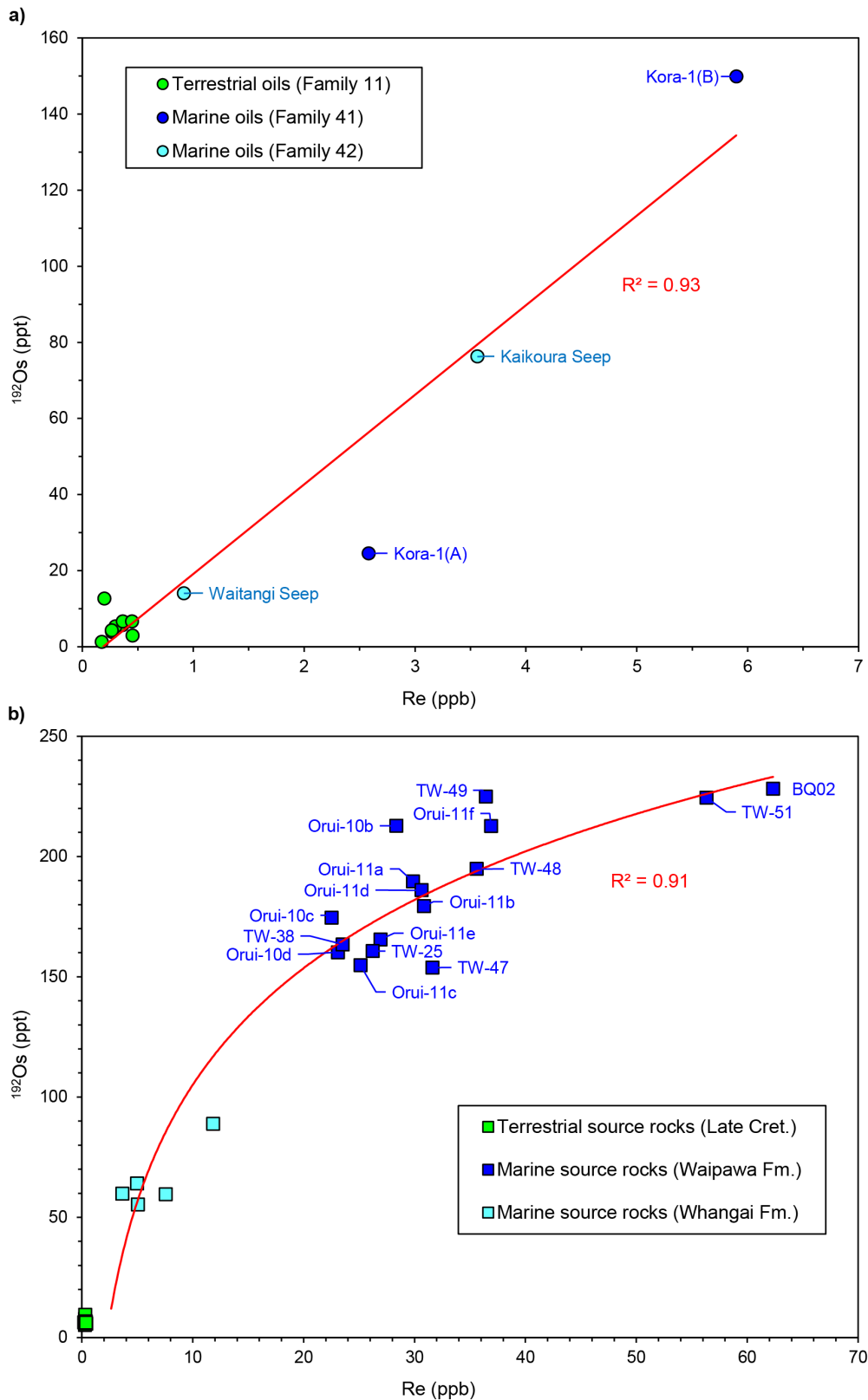
887

888 **Fig. 5.** Relative degree of water washing of the terrestrial and marine study oils
 889 indicated by cross-plots based on (a) C₆ to C₈ branched, cyclic and aromatic
 890 hydrocarbons, and (b) benzene and toluene aromatic hydrocarbons, *n*-hexane (*n*C₆)
 891 and *n*-heptane (*n*C₇). The Kaikoura Seep sample cannot be shown on either plot
 892 because of the major loss of C₆–C₈ hydrocarbons from biodegradation.



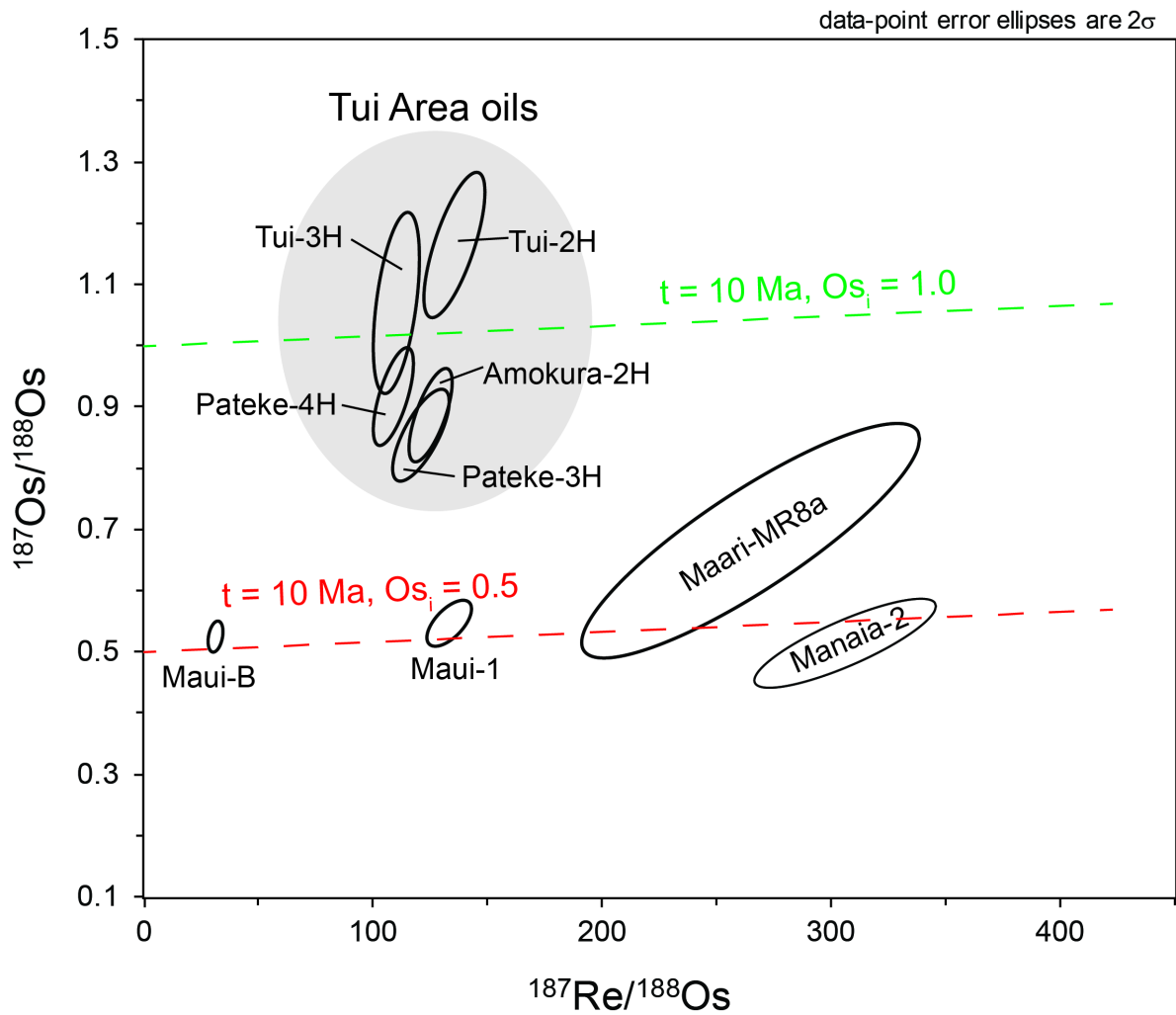
893

894 **Fig. 6.** Cross-plots of (a) Re and (b) ^{192}Os concentrations versus the asphaltene
 895 content of oils from families 11, 41 and 42.



896

897 **Fig. 7.** Cross-plots of Re and ^{192}Os concentrations in (a) the asphaltene fractions of
 898 terrestrial (Family 11) and marine oils (families 41 and 42) and b) their correlative or
 899 similar source rocks.

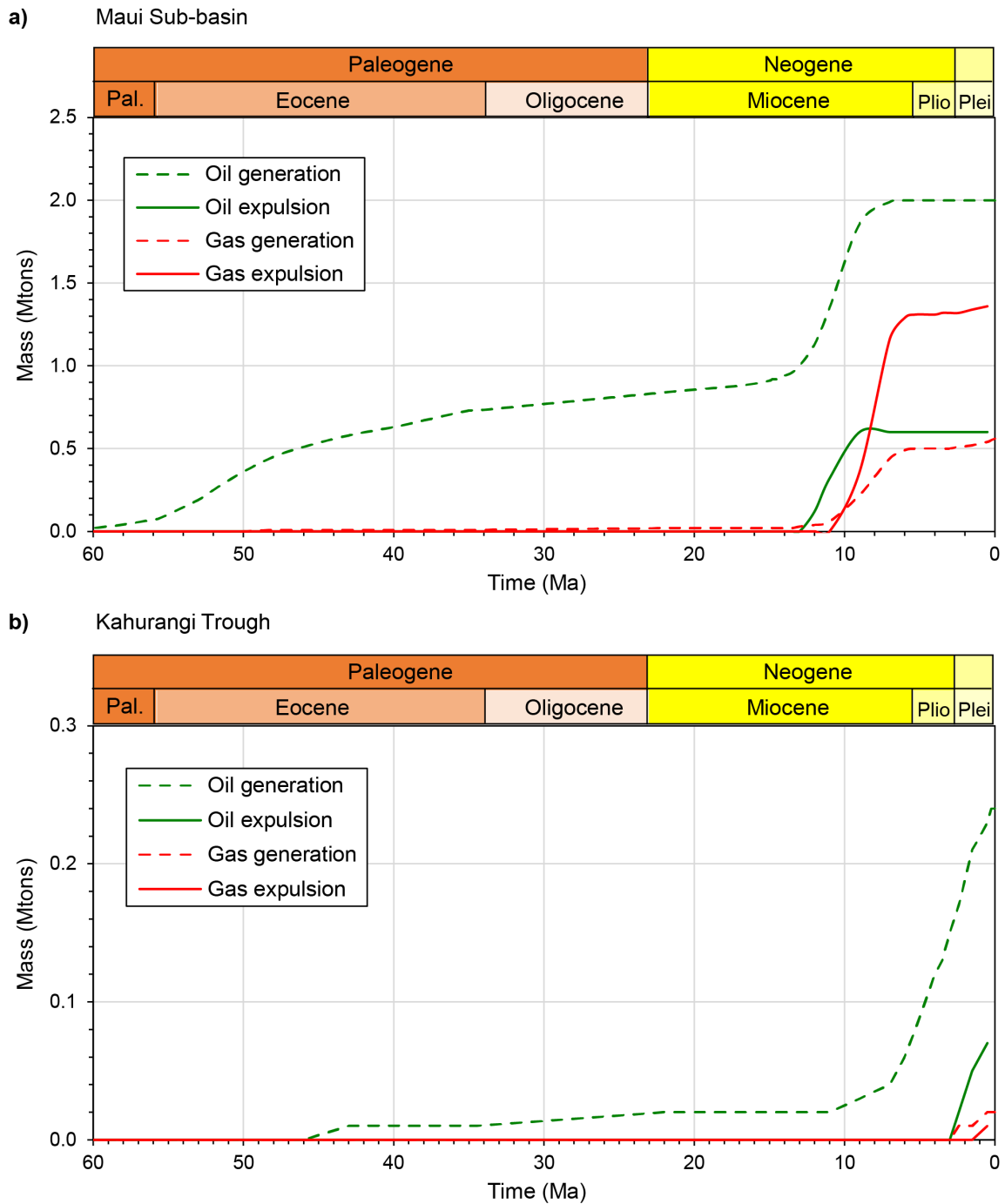


900

901 **Fig. 8.** $^{187}\text{Re}/^{188}\text{Os}$ versus $^{187}\text{Os}/^{188}\text{Os}$ for the asphaltene fractions of Family 11
 902 terrestrial oils from the Tui Area, Maui and Maari-Manaia fields. Uncertainty ellipses
 903 show the 2σ uncertainty. Reference lines with slopes equivalent to the timing of oil
 904 expulsion from the central Maui sub-basin and northern Kahurangi Trough ($\sim 10 \text{ Ma}$;
 905 Kroeger et al., 2021) and Os_i values of 0.5 and 1.0 are shown by the red and green
 906 dashed lines, respectively.

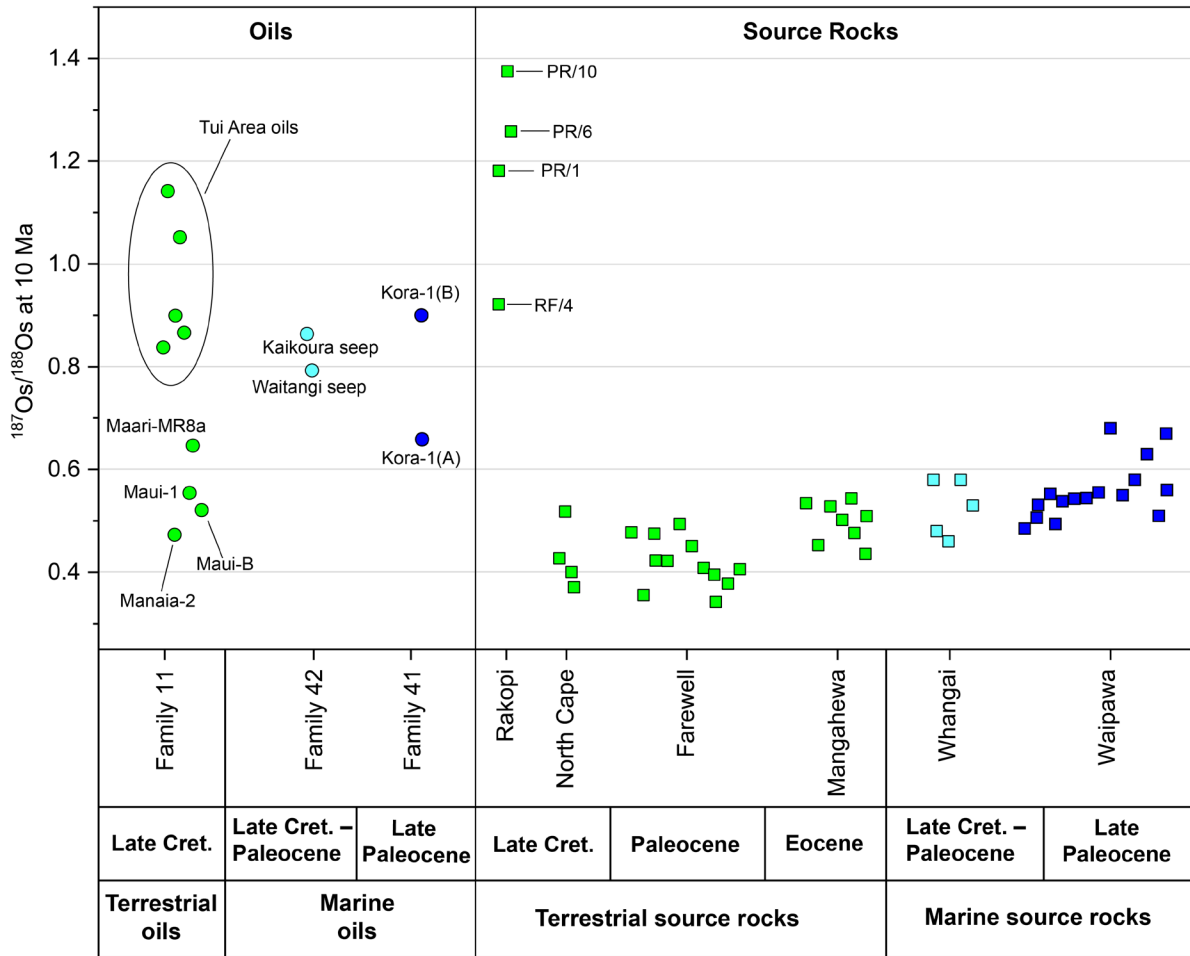
907

908



909

910 **Fig. 9.** Modelled oil and gas generation and expulsion histories of Late Cretaceous
 911 Rakopi Formation coaly source rocks at selected sites within the (a) central Maui
 912 sub-basin and (b) northern Kahurangi Trough. The models show cumulative mass (in
 913 megatons) per 200 x 200 m cell using organofacies D/E kerogen kinetics of Pepper
 914 and Corvi (1995a).



915

916 **Fig. 10.** Comparison of $^{187}\text{Os}/^{188}\text{Os}$ compositions at the time of oil expulsion
 917 (estimated to be ~10 Ma) for the terrestrial and marine oil families and their respective
 918 potential source rocks. The $^{187}\text{Os}/^{188}\text{Os}$ values for Farewell (Paleocene) and
 919 Mangahewa (Eocene) Formation coaly rocks are shown for comparison (data from
 920 Rotich et al., 2021).

921

- 923 Bischoff, A., Fensom, J., Tang, H., Rosetti, M., Nicol, A., 2021. Processes controlling
924 volcanic and epiclastic reservoir formation in a buried polygenetic stratocone.
925 In: Volcanic Processes in the Sedimentary Record: When Volcanoes Meet the
926 Environment. Di Capua A. (Ed.). The Geological Society Special Publications
927 SP520. DOI: 10.1144/SP520-2021-137.
- 928 Brett, W., 2005. Hydrocarbon potential of the Kora structure, PEP 38485. Ministry of
929 Economic Development, New Zealand, unpublished Petroleum Report 3346,
930 32 pp.
- 931 Bull, S., Hill, M.G., Strogen, D.P., Arnot, M.J., Seebeck, H., Kroeger, K.F., Zhu, H.,
932 2016. Seismic reflection interpretation, static modelling and velocity modelling
933 of the southern Taranaki Basin (4D Taranaki Project), GNS Science Report
934 2016/02, GNS Science, Lower Hutt. 91 p.
- 935 Christensen, J.N., Halliday, A.N., Leigh, K.E., Randell, R.N., Kesler, S.E., 1995. Direct
936 dating of sulfides by Rb-Sr: A critical test using the Polaris Mississippi Valley-
937 type Zn-Pb deposit. *Geochimica et Cosmochimica Acta*, 59: 519–5197.
- 938 Clayton, C., 2011. 3D Basin modelling of PEP 38485, offshore Taranaki Basin.
939 Ministry of Economic Development, New Zealand, unpublished Petroleum
940 Report 4313, 110 pp.
- 941 Cohen, A.S., Coe, A.L., Bartlett, J.M., Hawkesworth, C.J., 1999. Precise Re-Os ages
942 of organic-rich mudrocks and the Os isotope composition of Jurassic seawater.
943 *Earth and Planetary Science Letters*, 167: 159–173.
- 944 Colodner, D., Sachs, J., Ravizza, G., Turekian, K.K., Edmond, J., Boyle, E., 1993. The
945 geochemical cycle of rhenium: a reconnaissance. *Earth and Planetary Science
946 Letters*, 117: 205–221.
- 947 Corrick, A.J., Selby, D., McKirdy, D.M., Hall, P.A., Gong, S., Trefry, C., Ross, A.S.,
948 2019. Remotely constraining the temporal evolution of offshore oil systems.
949 *Scientific Reports*, 9: 1327.
- 950 Creaser, R.A., Papanastassiou, D.A., Wasserburg, G.J., 1991. Negative thermal ion
951 mass spectrometry of osmium, rhenium, and iridium. *Geochimica et
952 Cosmochimica Acta*, 55: 391–401.
- 953 Cumming, V.M., Selby, D., Lillis, P.G., 2012. Re-Os geochronology of the lacustrine
954 Green River Formation: Insights into direct depositional dating of lacustrine
955 successions, Re-Os systematics and paleocontinental weathering. *Earth and
956 Planetary Science Letters*, 359–360: 194–205.
- 957 Cumming, V.M., Selby, D., Lillis, P.G., Lewan, M.D., 2014. Re-Os geochronology and
958 Os isotope fingerprinting of petroleum sourced from a Type I lacustrine
959 kerogen: Insights from the natural Green River petroleum system in the Uinta
960 Basin and hydrous pyrolysis experiments. *Geochimica et Cosmochimica Acta*,
961 138: 32–56.
- 962 DiMarzio, J.M., Georgiev, S.V., Stein, H.J., Hannah, J.L., 2018. Residency of rhenium
963 and osmium in a heavy crude oil. *Geochimica et Cosmochimica Acta*, 220: 180–
964 200.
- 965 Field, B.D., Uruski, C.I., Beu, A.G., Browne, G.H., Crampton, J.S., Funnell, R.H.,
966 Killops, S.D., Laird, M., Mazengarb, C., Morgans, H.E.G., Rait, G.J., Smale, D.,
967 Strong, C.P., 1997. Cretaceous–Cenozoic geology and petroleum systems of
968 the East Coast region, New Zealand, Monograph 19, 7 enclosures. Institute of
969 Geological & Nuclear Sciences Limited, Lower Hutt, New Zealand, 301 pp.

- 970 Field, B.D., Naeher, S., Clowes, C.D., Shepherd, C.L., Hollis, C.J., Sykes, R., Ventura,
971 G.T., Pascher, K.M., Griffin, A.G., 2018. Depositional influences on the
972 petroleum potential of the Waipawa Formation in the Orui-1A drillhole,
973 Wairarapa. GNS Science report 2017/49, 75 pp.
- 974 Finlay, A. J., Selby, D., Osborne, M., Finucane, D., 2010. Fault charged mantle-fluid
975 contamination of North Sea oils: Insights from Re-Os isotopes. *Geology*, 38:
976 979-982.
- 977 Finlay, A.J., Selby, D., Osborne, M.J., 2011. Re-Os geochronology and fingerprinting
978 of United Kingdom Atlantic margin oil: Temporal implications for regional
979 petroleum systems. *Geology*, 39: 475–478.
- 980 Finlay, A.J., Selby, D., Osborne, M.J., 2012. Petroleum source rock identification of
981 United Kingdom Atlantic Margin oil fields and the Western Canadian Oil Sands
982 using Platinum, Palladium, Osmium and Rhenium: Implications for global
983 petroleum systems. *Earth and Planetary Science Letters*, 313–314: 95–104.
- 984 Funnell, R., Stagpoole, V.M., Nicol, A., Killops, S., Reyes, A.G., Darby, D., 2001.
985 Migration of oil and gas into the Maui Field, Taranaki Basin, New Zealand. In:
986 Hill, K.C., T., B. (Eds.), *Eastern Australasian Basins Symposium, A Refocused
987 Energy Perspective for the Future*. Petroleum Exploration Society of Australia,
988 pp. 121–128.
- 989 Funnell, R., Stagpoole, V.M., Nicol, A., McCormack, N., Reyes, A.G., 2004. Petroleum
990 generation and implications for migration: a Maui Field charge study, Taranaki
991 Basin, 2004 New Zealand Petroleum Conference Proceedings. Ministry of
992 Business, Innovation & Employment (MBIE), New Zealand unpublished
993 petroleum report PR5005, 9 pp.
- 994 Ge, X., Shen, C., Selby, D., Deng, D., Mei, L., 2016. Apatite fission-track and Re-Os
995 geochronology of the Xuefeng uplift, China: Temporal implications for dry gas
996 associated hydrocarbon systems. *Geology*, 44: 491–494.
- 997 Ge, X., Shen, C., Selby, D., Wang, J., Ma, L., Ruan, X., Hu, S., Mei, L., 2018.
998 Petroleum-generation timing and source in the northern Longmen Shan thrust
999 belt, Southwest China: Implications for multiple oil-generation episodes and
1000 sources. *American Association of Petroleum Geologists Bulletin*, 102: 913–938.
- 1001 Georgiev, S.V., Stein, H.J., Hannah, J.L., Galimberti, R., Nali, M., Yang, G.,
1002 Zimmerman, A., 2016. Re-Os dating of maltenes and asphaltenes within single
1003 samples of crude oil. *Geochimica et Cosmochimica Acta*, 179: 53–75.
- 1004 Georgiev, S.V., Stein, H.J., Hannah, J.L., Yang, G., Markey, R.J., Dons, C.E.,
1005 Pedersen, J.H., di Primio, R., 2019. Comprehensive evolution of a petroleum
1006 system in absolute time: The example of Brynhild, Norwegian North Sea.
1007 *Chemical Geology*, 522: 260–282.
- 1008 Goldstein, T.P., Aizenshtat, Z., 1994. Thermochemical sulfate reduction a review.
1009 *Journal of Thermal Analysis*, 42: 241–290.
- 1010 Goswami, V., Hannah, J.L., Stein, H.J., 2018. Why terrestrial coals cannot be dated
1011 using the Re-Os geochronometer: Evidence from the Finnmark Platform,
1012 southern Barents Sea and the Fire Clay coal horizon, Central Appalachian
1013 Basin. *International Journal of Coal Geology*, 188: 121–135.
- 1014 Harrison, A., Reid, E., Smith, N., 2013. PEP 51906 Seismic Interpretation Report.
1015 Ministry of Business, Innovation and Employment, New Zealand, unpublished
1016 Petroleum Report 4664, 79 pp.
- 1017 Higgs, K.E., King, P.R., Raine, J.I., Sykes, R., Browne, G.H., Crouch, E.M., Baur, J.R.,
1018 2012. Sequence stratigraphy and controls on reservoir sandstone distribution
1019 in an Eocene marginal marine-coastal plain fairway, Taranaki Basin, New
1020 Zealand. *Marine and Petroleum Geology* 32, 110-137.

- 1021 Hnatyshin, D., 2018. Development and application of the Re-Os isotope system to
1022 sediment-hosted Zn-Pb ores and sedimentary pore waters (Doctoral thesis,
1023 University of Alberta, Edmonton, Canada). <https://doi.org/10.7939/R31G0J990>
- 1024 Hollis, C.J., Manzano-Kareah, K., 2005. Source rock potential of the East Coast Basin.
1025 Ministry of Economic Development New Zealand, unpublished Petroleum
1026 Report 3179, 158 pp.
- 1027 Hurtig, N.C., Georgiev, S.V., Stein, H.J., Hannah, J.L., 2019. Re-Os systematics in
1028 petroleum during water-oil interaction: The effects of oil chemistry. *Geochimica*
1029 *et Cosmochimica Acta*, 247: 142–161.
- 1030 Killops, S., 1996. A geochemical perspective of oil generation in New Zealand basins,
1031 1996 New Zealand Petroleum Conference, proceedings, Volume, 1, 179–187.
1032 Ministry of Business, Innovation & Employment (MBIE), New Zealand
1033 unpublished petroleum report PR5001.
- 1034 Killops, S.D., Woolhouse, A.D., Weston, R.J., Cook, R.A., 1994. A geochemical
1035 appraisal of oil generation in the Taranaki Basin, New Zealand. *American*
1036 *Association of Petroleum Geologists Bulletin*, 78: 1560–1584.
- 1037 King, P.R., Thrasher, G.P., 1996. Cretaceous–Cenozoic geology and petroleum
1038 systems of the Taranaki Basin, New Zealand, Monograph 13. Institute of
1039 Geological & Nuclear Sciences Limited, 243 pp.
- 1040 Kroeger, K.F., Plaza-Faverola, A., Barnes, P.M., Pecher, I.A., 2015. Thermal evolution
1041 of the New Zealand Hikurangi subduction margin: Impact on natural gas
1042 generation and methane hydrate formation – A model study. *Marine and*
1043 *Petroleum Geology* 63, 97-114.
- 1044 Kroeger, K., Funnell, R., Arnot, M., Bull, S., Hill, M., Sahoo, T., Zhu, H., 2016. Re-
1045 assessment of maturity and charge in southern Taranaki Basin (New Zealand)
1046 using integrated 3D basin modelling, AAPG/SEG International Conference &
1047 Exhibition 2015. Eastern Australian Basins Symposium, Melbourne, Australia,
1048 pp. 217–230.
- 1049 Kroeger, K.F., Thrasher, G.P., Sarma, M., 2019. The evolution of a Middle Miocene
1050 deep-water sedimentary system in northwestern New Zealand (Taranaki
1051 Basin): Depositional controls and mechanisms. *Marine and Petroleum Geology*
1052 101, 355-372.
- 1053 Kroeger, K.F., Seebeck, H., Thrasher, G.P., Arnot, M., Bull, S., Viskovic, G.P.D., 2021.
1054 Reconstruction of rapid charge of a giant gas field across a major fault zone
1055 using 3D petroleum systems modelling (Taranaki Basin, New Zealand). *Marine*
1056 *and Petroleum Geology*, 130: 105121.
- 1057 Kroeger, K.F., Bischoff, A., Nicol, A., 2022. Petroleum systems in a buried
1058 stratovolcano: Maturation, migration and leakage. *Marine and Petroleum*
1059 *Geology* 141, 105682.
- 1060 Lassiter, J.C., Luhr, J.F., 2001. Osmium abundance and isotope variations in mafic
1061 Mexican volcanic rocks: Evidence for crustal contamination and constraints on
1062 the geochemical behavior of osmium during partial melting and fractional
1063 crystallization. *Geochemistry, Geophysics, Geosystems*, 2: 1027.
- 1064 Levorsen, A.I., 2001. *Geology of Petroleum*. American Association of Petroleum
1065 Geologists Bulletin, Special Publication, Oklahoma, 724 pp.
- 1066 Lillis, P.G., Selby, D., 2013. Evaluation of the rhenium-osmium geochronometer in the
1067 Phosphoria petroleum system, Bighorn Basin of Wyoming and Montana, USA.
1068 *Geochimica et Cosmochimica Acta*, 118: 312–330.
- 1069 Liu, J., Pearson, D.G., 2014. Rapid, precise and accurate Os isotope ratio
1070 measurements of nanogram to sub-nanogram amounts using multiple Faraday

1071 collectors and amplifiers equipped with 1012 Ω resistors by N-TIMS. *Chemical*
1072 *Geology*, 363: 301–311.

1073 Liu, J., Selby, D., Obermajer, M., Mort, A., 2018. Rhenium–osmium geochronology
1074 and oil–source correlation of the Duvernay petroleum system, Western Canada
1075 sedimentary basin: Implications for the application of the rhenium–osmium
1076 geochronometer to petroleum systems. *American Association of Petroleum*
1077 *Geologists Bulletin*, 102: 1627–1657.

1078 Liu, J., Selby, D., Zhou, H., Pujol, M., 2019. Further evaluation of the Re-Os
1079 systematics of crude oil: Implications for Re-Os geochronology of petroleum
1080 systems. *Chemical Geology*, 513: 1–22.

1081 Magoon, L.B., Dow, W.G., 1994. *The Petroleum System—From Source to Trap*, 60.
1082 *American Association of Petroleum Geologists Bulletin*, Oklahoma, 644 pp.

1083 Mahdaoui, F., Reisberg, L., Michels, R., Hautevelle, Y., Poirier, Y., Girard, J.P., 2013.
1084 Effect of the progressive precipitation of petroleum asphaltenes on the Re-Os
1085 radioisotope system. *Chemical Geology*, 358: 90–100.

1086 Mahdaoui, F., Michels, R., Reisberg, L., Pujol, M., Poirier, Y., 2015. Behavior of Re
1087 and Os during contact between an aqueous solution and oil: Consequences for
1088 the application of the Re-Os geochronometer to petroleum. *Geochimica et*
1089 *Cosmochimica Acta*, 158: 1–21.

1090 Mark, D.F., Parnell, J., Kelley, S.P., Lee, M.R., Sherlock, S.C., 2010. $^{40}\text{Ar}/^{39}\text{Ar}$ dating
1091 of oil generation and migration at complex continental margins: *Geology*, 38:
1092 75–78.

1093 Matthews, E.R., 2002. Implications of Neogene structural development on
1094 hydrocarbon prospectivity of the Tui-Maui area, offshore Taranaki Basin, New
1095 Zealand., 2002 NZ Petroleum Conference Proceedings. Ministry of Business,
1096 Innovation & Employment (MBIE), New Zealand unpublished petroleum report
1097 PR5004.

1098 Matthews, E.R., 2008. AWE Taranaki Exploration. 2008 NZ Petroleum Conference
1099 Proceedings. Ministry of Business, Innovation & Employment (MBIE), New
1100 Zealand unpublished petroleum report PR5007.

1101 Matthews, E.R., Kunjan, B., Osman, N., Shadlow, J., John, Z., Spotkoeff, M., Saicic,
1102 M., 2008. Tui Fields Geoscience Review, 2008 New Zealand Petroleum
1103 Conference Proceedings. Ministry of Business, Innovation & Employment
1104 (MBIE), New Zealand unpublished petroleum report PR5007.

1105 Meng, Q., Wang X., Huo, Q., Dong, Z., Li, Z., Tesselina, S.G., Ware, B.D., McInnes,
1106 B.A., Wang, X., Liu, T., Zhang, L., 2021. Rhenium–osmium (Re-Os)
1107 geochronology of crude oil from lacustrine source rocks of the Hailar Basin, NE
1108 China. *Petroleum Science*, 18: 1-9

1109 [MBIE] Ministry of Business, Innovation & Employment, 2020. Energy in New Zealand
1110 2020. [https://www.mbie.govt.nz/building-and-energy/energy-and-natural-
1111 resources/energy-statistics-and-modelling/energy-publications-and-technical-
1112 papers/energy-in-new-zealand/](https://www.mbie.govt.nz/building-and-energy/energy-and-natural-resources/energy-statistics-and-modelling/energy-publications-and-technical-papers/energy-in-new-zealand/) (accessed January 2022).

1113 Moore, P.R., 1989. Stratigraphy of the Waipawa Black Shale (Paleocene), eastern
1114 North Island, New Zealand. *New Zealand Geological Survey record*, 38, 19 pp.

1115 Murray, A.P., Summons, R.E., Boreham, C.J., Reed, J.D., Francis, D.A., 1994.
1116 Geochemistry of oils and source rocks of the East Coast Basin and implications
1117 for the Taranaki Basin, New Zealand., 1994 New Zealand petroleum
1118 conference proceedings. Ministry of Business, Innovation & Employment
1119 (MBIE), New Zealand unpublished petroleum report PR5000, Wellington, pp.
1120 338–351.

- 1121 Naeher, S., Hollis, C.J., Clowes, C.D., Ventura, G.T., Shepherd, C.L., Crouch, E.M.,
1122 Morgans, H.E.G., Bland, K.J., Strogon, D.P., Sykes, R., 2019. Depositional and
1123 organofacies influences on the petroleum potential of an unusual marine source
1124 rock: Waipawa Formation (Paleocene) in southern East Coast Basin, New
1125 Zealand. *Marine and Petroleum Geology*, 104: 468–488.
- 1126 [NZOP] New Zealand Overseas Petroleum Limited, 2005. Tui Area Mining Permit
1127 Application - Technical Data. Ministry of Economic Development, New Zealand
1128 unpublished petroleum report PR3223, pp. 824.
- 1129 Palmer, S.E., 1984. Effect of water washing on C₁₅₊ hydrocarbon fractions of crude
1130 oils from Northwest Palawan, Philippines. *American Association of Petroleum
1131 Geologists Bulletin*, 68: 137–149.
- 1132 Paul, M., Reisberg, L., Vigier, N., Zheng, Y., Ahmed, K.M., Charlet, L., Huq, M.R.,
1133 2010. Dissolved osmium in Bengal plain groundwater: Implications for the
1134 marine Os budget. *Geochimica et Cosmochimica Acta*, 74: 3432–3448.
- 1135 Pepper, A.S., 1991. Estimating the petroleum expulsion behaviour of source rocks: a
1136 novel quantitative approach. Geological Society, London, Special Publications,
1137 59: 9–31.
- 1138 Pepper, A.S., Corvi, P.J., 1995a. Simple kinetic models of petroleum formation. Part
1139 I: oil and gas generation from kerogen. *Marine and Petroleum Geology*, 12:
1140 291–319.
- 1141 Pepper, A.S., Corvi, P.J., 1995b. Simple kinetic models of petroleum formation. Part
1142 III: Modelling an open system. *Marine and Petroleum Geology*, 12: 417–452.
- 1143 Peters, K.E., Cassa, M.R., 1994. Applied source rock geochemistry. In: Magoon, L.B.,
1144 Dow, W.G. (Eds.), *The Petroleum System: From Source to Trap*. American
1145 Association of Petroleum Geologists Memoir, pp. 93–120.
- 1146 Peters, K E, and Moldowan, J M. 1993. *The biomarker guide: Interpreting molecular
1147 fossils in petroleum and ancient sediments*. Englewood Cliffs, Prentice Hall, 363
1148 pp.
- 1149 Peters, K.E., Walters, C.C., Moldowan, J.M., 2005. *The Biomarker Guide: Volume 2:
1150 Biomarkers and Isotopes in Petroleum Systems and Earth History*, 2.
1151 Cambridge University Press, Cambridge, 700 pp.
- 1152 Peucker-Ehrenbrink, B., Ravizza, G., 2012. Chapter 8 - Osmium Isotope Stratigraphy.
1153 In: Gradstein, F.M., Ogg, J.G., Schmitz, M.D., Ogg, G.M. (Eds.), *The Geologic
1154 Time Scale*. Elsevier, Boston, pp. 145–166.
- 1155 Pierpont, R., Wunderlich, A., Mayer, J., 2017. PEP 60089 Petroleum system and
1156 migration interpretation report. Ministry of Business, Innovation and
1157 Employment, New Zealand, unpublished Petroleum Report 5514, 22 pp.
- 1158 Reed, J.D., 1992. Exploration geochemistry of the Taranaki Basin with emphasis on
1159 Kora, 1991 New Zealand Oil Exploration Conference Proceedings. Ministry of
1160 Commerce, pp. 364–372
- 1161 Reilly, C., Nicol, A., Walsh, J.J., Kroeger, K.F., 2016. Temporal changes of fault seal
1162 and early charge of the Maui Gas-condensate field, Taranaki Basin, New
1163 Zealand. *Marine and Petroleum Geology*, 70: 237–250.
- 1164 Rodushkin, I., Engström, E., Sörlin, D., Pontèr, C., Baxter, D.C., 2007. Osmium in
1165 environmental samples from Northeast Sweden: Part I. Evaluation of
1166 background status. *Science of the Total Environment*, 386: 145–158.
- 1167 Rogers, K.M., Collen, J.D., Johnston, J.H., Elgar, N.E., 1999. A geochemical appraisal
1168 of oil seeps from the East Coast Basin, New Zealand. *Organic Geochemistry*,
1169 30: 593–605.
- 1170 Rooney, A.D., Selby, D., Lewan, M.D., Lillis, P.G., Houzay, J.P., 2012. Evaluating Re-
1171 Os systematics in organic-rich sedimentary rocks in response to petroleum

1172 generation using hydrous pyrolysis experiments. *Geochimica et Cosmochimica*
1173 *Acta*, 77: 275–291.

1174 Rotich, E.K., Handler, M.R., Naeher, S., Selby, D., Hollis, C.J., Sykes, R., 2020. Re-
1175 Os geochronology and isotope systematics, and organic and sulfur
1176 geochemistry of the middle–late Paleocene Waipawa Formation, New Zealand:
1177 Insights into early Paleogene seawater Os isotope composition. *Chemical*
1178 *Geology*, 536: 119473.

1179 Rotich, E.K., Handler, M.R., Sykes, R., Selby, D., Naeher, S., 2021. Depositional
1180 influences on Re-Os systematics of Late Cretaceous–Eocene fluvio-deltaic
1181 coals and coaly mudstones, Taranaki Basin, New Zealand. *International*
1182 *Journal of Coal Geology*, 236: 103670.

1183 Scarlett, A.G., Holman, A.I., Georgiev, S.V., Stein, H.J., Summons, R.E., Grice, K.,
1184 2019. Multi-spectroscopic and elemental characterization of southern
1185 Australian asphaltites. *Organic Geochemistry*, 133: 77–91.

1186 Schiøler, P., Rogers, K.M., Sykes, R., Hollis, C.J., Ilg, B., Meadows, D., Roncaglia, L.,
1187 Uruski, C.I., 2010. Palynofacies, organic geochemistry and depositional
1188 environment of the Tartan Formation (Late Paleocene), a potential source rock
1189 in the Great South Basin, New Zealand. *Marine and Petroleum Geology*, 27:
1190 351–369.

1191 Schlumberger, 2017. 1D Petroleum system modelling onshore East Coast Basin, New
1192 Zealand. Ministry of Business, Innovation and Employment, New Zealand,
1193 unpublished Petroleum Report 5404, 43 pp.

1194 Seebeck, H., Thrasher, G.P., Viskovic, G.P., 2019. Inversion history of the northern
1195 Tasman Ridge, Taranaki Basin, New Zealand: implications for petroleum
1196 migration and accumulation. *New Zealand Journal of Geology and Geophysics*,
1197 63: 299–323.

1198 Selby, D., Creaser, R.A., 2005. Direct radiometric dating of hydrocarbon deposits
1199 using rhenium-osmium isotopes. *Science*, 308: 1293–1295.

1200 Selby, D., Creaser, R.A., Dewing, K., Fowler, M., 2005. Evaluation of bitumen as a
1201 ^{187}Re - ^{187}Os geochronometer for hydrocarbon maturation and migration: A test
1202 case from the Polaris MVT deposit, Canada. *Earth and Planetary Science*
1203 *Letters*, 235: 1–15.

1204 Selby, D., Creaser, R.A., Fowler, M.G., 2007. Re-Os elemental and isotopic
1205 systematics in crude oils. *Geochimica et Cosmochimica Acta*, 71: 378–386.

1206 Smith, N., Wunderlich, A., Mallinson, I., 2016. PEP 51313 - Stage 2 Prospectivity
1207 Interpretation Report. Ministry of Business, Innovation & Employment (MBIE),
1208 New Zealand unpublished petroleum report PR5332.

1209 Speight, J.G., 2004. Petroleum asphaltenes – part 1: Asphaltenes, resins and the
1210 structure of petroleum. *Oil & Gas Science and Technology*, 59: 467–477.

1211 Stagpoole, V., Nicol, A., 2008. Regional structure and kinematic history of a large
1212 subduction back thrust: Taranaki Fault, New Zealand. *Journal of Geophysical*
1213 *Research: Solid Earth*, 113: B01403.

1214 Suzuki, K., Tatsumi, Y., 2006. Re-Os systematics of high-Mg andesites and basalts
1215 from the Setouchi volcanic belt, SW Japan: Implications for interaction between
1216 wedge mantle and slab-derived melt. *Geochemical Journal*, 40: 297–307.

1217 Sykes, R., Andrew, S.M., Joanne, C., 2011. The New Zealand Petroleum PVT
1218 Database. GNS Science Data Series 8a. Ministry of Economic Development,
1219 New Zealand unpublished petroleum report PR4519.

1220 Sykes, R., Zink, K.-G., Rogers, K.M., Phillips, A., Ventura, G.T., 2012. New and
1221 updated geochemical databases for New Zealand petroleum samples, with
1222 assessments of genetic oil families, source age, facies and maturity. GNS

1223 Science consultancy report 2012/37, Ministry of Economic Development, New
1224 Zealand unpublished petroleum report PR4513, 29 pp.

1225 Sykes, R., Volk, H., George, S.C., Ahmed, M., Higgs, K.E., Johansen, P.E., Snowdon,
1226 L.R., 2014. Marine influence helps preserve the oil potential of coaly source
1227 rocks: Eocene Mangahewa Formation, Taranaki Basin, New Zealand. *Organic*
1228 *Geochemistry*, 66: 140–163.

1229 Sykes, R., Zink, K.-G., 2018. The New Zealand Oils Geochemistry Database (Version
1230 2.0). GNS Science Data Series 24a. <https://data.gns.cri.nz/pbe/>.

1231 Sykes, R., 2019. Chemometric classification of terrestrial oil families in Taranaki Basin,
1232 New Zealand: higher plant trends and migration contamination effects. *AAPG*
1233 *Datapages*, #30628. [http://www.searchanddiscovery.com/documents/2019/30](http://www.searchanddiscovery.com/documents/2019/30628sykes/ndx_sykes.pdf)
1234 [628sykes/ndx_sykes.pdf](http://www.searchanddiscovery.com/documents/2019/30628sykes/ndx_sykes.pdf).

1235 Symons, D.T.A., Arne, D.C., 2003. Paleomagnetic dating of mineralization in the
1236 Kapok MVT deposit, Lennard Shelf, Western Australia. *Journal of Geochemical*
1237 *Exploration*, 78-79, 267–272.

1238 Tripathy, G.R., Hannah, J.L., Stein, H.J., and Yang, G., 2014. Re-Os age and
1239 depositional environment for black shales from the Cambrian-Ordovician
1240 boundary, Green Point, western Newfoundland: *Geochemistry, Geophysics,*
1241 *Geosystems*, 15: 1021–1037.

1242 van Acken, D., Tütken, T., Daly, J.S., Schmid-Röhl, A., Orr, P.J., 2019.
1243 Rhenium-osmium geochronology of the Toarcian Posidonia Shale, SW
1244 Germany. *Palaeogeography, Palaeoclimatology, Palaeoecology*, 534: 109294.

1245 Walters, C.C., Wang, F.C., Qian, K., Wu, C., Mennito, A.S., Wei, Z., 2015. Petroleum
1246 alteration by thermochemical sulfate reduction – A comprehensive molecular
1247 study of aromatic hydrocarbons and polar compounds. *Geochimica et*
1248 *Cosmochimica Acta*, 153: 37–71.

1249 Wang, G., Xue, Y., Wang, D., Shi, S., Grice, K., Greenwood, P.F., 2016.
1250 Biodegradation and water washing within a series of petroleum reservoirs of
1251 the Panyu Oil Field. *Organic Geochemistry*, 96: 65–76.

1252 Wenger, L.M., Davis, C.L., Isaksen, G.H., 2002. Multiple Controls on Petroleum
1253 Biodegradation and Impact on Oil Quality. *SPE Reservoir Evaluation &*
1254 *Engineering*, 5: 375–383.

1255 Wilkins, R.W.T., George, S.C., 2002. Coal as a source rock for oil: a review.
1256 *International Journal of Coal Geology*, 50: 317–361.

1257 Xu, G., Hannah, J.L., Stein, H.J., Bingen, B., Yang, G., Zimmerman, A., Weitschat,
1258 W., Mørk, A., Weiss, H.M., 2009. Re-Os geochronology of Arctic black shales
1259 to evaluate the Anisian–Ladinian boundary and global faunal correlations: *Earth*
1260 *and Planetary Science Letters*, 288: 581–587.

1261 Zhao, C., Cheng, K., 1998. Expulsion and primary migration of the oil derived from
1262 coal. *Science in China Series D: Earth Sciences*, 41: 345–353.

1263
1264